

CHAPTER 1

INTRODUCTION

This chapter provides a background to this study, the research outline, problem statement, hypotheses, research aim and specific objectives.

1.1 BACKGROUND

Over 70% of the Earth's surface is covered by water; most of it is unsuitable for human consumption. Freshwater lakes, rivers and underground aquifers represent only 2.5% of the world's total freshwater supply. Unfortunately, in addition to being scarce, clean water is also very unevenly distributed. Fresh and clean water availability is equally important for people, animals and agricultural activities. The world, unfortunately is facing formidable challenges in meeting rising demands for clean water as the available supplies of freshwater are decreasing due to population growth, more stringent health-based regulations, competing demands from a variety of users, extended droughts and contamination of water resources with pathogenic bacteria (Oves *et al.* 2015).

Presently, water disinfection is carried out through different techniques such as chlorination, UV treatment and ozonisation, but these disinfection routes have limitations for large scale implementation. Conventional treatment technologies have shown limited ability in reducing the high levels of pathogenic bacteria in water. It is therefore crucial to develop sustainable technologies that will address these problems as the ability to recycle and reuse water would be of great benefit to both industries and the environment. Nano material applications open the door to improve the waste treatment methods. This includes decontamination of the finest contaminants in water due to its large reactive surface and induced coatings of pollutants that

can reduce the toxicity and kill pathogens. Hence, nanotechnology creates new opportunities to reduce or kill the pathogenic bacteria in water (Oves *et al.* 2015).

Nanotechnology is the science of the production, manipulation and use of materials at the subatomic level. A nanoparticle is a small object that behaves as a whole unit in terms of its transport and properties. Ultrafine particles are sized between 1 and 100 nm (Gosmann and Feldman 2010). In recent years, noble metal oxide nanoparticles have been the subject of focused research due to their unique electronic, optical, mechanical, magnetic and chemical properties that are significantly different from those of its bulk counterparts (Kumarl & Sangwan 2011). Nanostructured metal oxides such as ZnO and Co₃O₄, have recently received attention because of their antibacterial activity, stability and safety for humans and ecosystems.

Zinc oxide nanoparticles are at the forefront of research due to their unique properties such as semiconduction, antibacterial and antifungal activity in wound healing. ZnO nanoparticles were added to the wallpapers of hospitals to overcome the microbial load on walls and prevent nosocomial infection. Mechanistically the antimicrobial activity of ZnO was enhanced due to the presence of water molecules on its surface. These aqueous suspensions of ZnO and water generate free radicals of hydroxyl and oxygen species which are responsible for remarkable oxidative stress in treated bacterial cells (Jurablu *et al.* 2015).

There are three techniques used for the preparation of ZnO nanopowders: sol-gel method, coprecipitation method and urea-based synthesis. The sol-gel approach appears to be one of the most promising methods to prepare ZnO nanoparticles. The advantages of the sol-gel method are ease of synthesis, low temperature of decomposition and control in the chemical composition. They make the sol-gel technique a very attractive preparation method, especially in the case of photocatalytically active ZnO powders (Jurablu *et al.* 2015).

On the other hand, cobalt oxide nanoparticles play an important role as antimicrobial agents and can be used because of its effectiveness against resistant strains of microbial pathogens, lower toxicity and heat resistance (Karvani and Chehrazi 2011). The properties of Co_3O_4 are highly related to particle size. Much effort has been made to prepare Co_3O_4 nanoparticles, including pulsed laser deposition, sol-gel route and reduction-oxidation route. However, nanocrystalline Co_3O_4 is more difficult and inconvenient to obtain (Yang *et al.* 2003).

In this research project, the synthesis of Co_3O_4 and ZnO nanoparticles by mechano-chemical and sol-gel methods will be investigated and tested against selected waterborne pathogenic fungi (yeasts and moulds), protozoa and bacteria. The nanoparticles were characterized by the following techniques: Ultraviolet-visible (UV- Vis) Spectroscopy, Fourier Infrared Spectroscopy (FTIR), Transmission Electron Microscopy (TEM) and Scanning Electron Microscopy (SEM).

1.2. RATIONALE / MOTIVATION

Recently antibiotics have been used to such a degree that bacteria are becoming resistant to them. Due to the growing concern regarding multidrug resistant bacterial infections, alternative treatment needs to be exploited. The use of nanoparticles can compensate for the failure of antibiotics and it will serve as an alternative process to treat lethal infectious diseases. Various types of oxide based nanomaterials are an attractive option for the disinfection of water due to its high chemical stability and non-toxicity towards human cells (Yang *et al.* 2003).

1.3. PROBLEM STATEMENT

Microbial contamination of water is a great risk for human health. Globally, millions of people are facing a huge scarcity of water supply. It is predicted that nearly 1.8 billion people will face water scarcity by 2025. Most of the diseases occurring in developing countries are due to

consumption of contaminated water. Therefore, in order to solve this problem, there is a need to develop effective antimicrobial agents to control the growth of microbial populations in water. Nanotechnology offers a way to develop alternative antimicrobial agents for water purification (Tang and Bin- Feng 2014).

1.4. AIM

The aim of the study is to synthesise, characterize and assess the antimicrobial activity of cobalt oxide, zinc oxide and cobalt-doped zinc oxide nanoparticles against selected waterborne pathogenic fungi (yeasts and moulds) and bacteria.

1.5. OBJECTIVES

1. To synthesise ZnO nanoparticles using urea-based synthesis method
2. To synthesise Co₃O₄ nanoparticles using mechano-chemical and sol-gel methods
3. To synthesise Co₃O₄-doped ZnO nanoparticles using chemical synthesis method
4. To characterise the nanoparticles using Ultraviolet-visible (UV- Vis) Spectroscopy, Fourier Infrared Spectroscopy (FTIR), Transmission Electron Microscopy (TEM) and Scanning Electron Microscopy (SEM)
5. To test for antimicrobial activities of these nanoparticles on pathogenic fungi (yeasts and moulds) and bacteria using MIC and disc diffusion
6. To perform toxicity test for synthesised nanoparticles using *Daphnia magna* (Daphtox kit)

1.6. THESIS OUTLINE

This dissertation is organised into five chapters:

Chapter Two contains a detailed description of literature of the study. It provides an account of the fundamental principles and applications relating to the research conducted and published by other researchers.

Chapter Three provides details on the methods employed. The materials used, the research design, the analytical techniques and the instrumentation used.

Chapters Four includes the characterisation results and discussion.

Chapter Five includes antimicrobial and toxicity results

Chapter Six provides the general conclusion and recommendations.

Chapter Seven is the list of all references used to compile the study.

CHAPTER 2

LITERATURE REVIEW

This chapter provides an account of the fundamental principles and applications relating to the research conducted and published by other researchers. The literature review presented in this chapter focuses on the water shortage, water pollution, characterisation and antimicrobial activities of nanoparticles.

2.1. Waterborne pathogens

Bacteria are found everywhere including air, soil, plants and water, while others live in or on other organisms like animals and humans. A relatively few of these bacteria are parasitic and pathogenic, causing diseases such as cholera, typhoid fever, dysentery, and other illnesses in humans. Most pathogenic bacteria are introduced to water sources by human and animal waste, and then grow in water and initiate infection in the gastrointestinal tract after ingestion. However, bacteria such as *Legionella* are environmental microorganisms that can grow in soil and water (Wenneras *et al.* 2004). Besides ingestion, bacterial transmission can occur through inhalation and contact; leading to infections to the respiratory tract and skin, respectively. Bacterial contaminants that are commonly found in drinking water include *Salmonella*, *Shigella*, *Vibrio cholerae* and some strains of *Escherichia coli* (Wenneras *et al.* 2004)..

2.1.1 *Escherichia coli*

Escherichia coli (*E. coli*) is a very widely studied bacteria. They are common gram negative bacteria that are generally not harmful. Some of these bacterial strains are used as indicator organisms to monitor the presence and quality of other biological contaminants in drinking

water. However, pathogenic *E. coli* strains such as Enterotoxigenic Escherichia coli (ETEC) is one of the leading causes of diarrhoea in developing countries. It has been estimated that each year approximately 840 million cases and 380 000 death occur, mostly in children, due to this bacterial infection (Jafari *et al.* 2008; Cabral 2010).

2.1.2. *Vibrio cholerae*

Vibrio cholerae (*V. cholerae*) are small comma-shaped, gram negative bacteria. The cells of *V. cholerae* grow at temperatures of around 40 °C and pH of 9-11. This bacterium is the main cause of the epidemic cholera. The disease is characterised by acute and very intense diarrhoea. In developing countries, children under 5 years are affected by this disease, which has been characterised to be the main cause of death transmitted through bacterial contaminated water (All Africa 2014). A recent cholera outbreak has been reported in Ghana where it claimed more than 100 lives and over 11 000 cases were reported by September 2014. Other cholera outbreaks have been reported in multiple African countries including Nigeria, Somalia, Democratic Republic of Congo, Zambia, Sierra Leone, etc., between 2010 and 2014 (Vaccine News Daily 2014).

2.1.3. *Salmonella*

Salmonella is a rod-shaped, gram negative bacterium. Typhoid fever is caused by *Salmonella*. The disease has been found to pass from humans to animals and vice versa through drinking contaminated water. A low dosage of the bacteria in the water is enough to cause clinical symptoms. The non-typhoidal *Salmonella* rarely causes waterborne outbreaks but the *Salmonella typhi* causes large and devastating outbreaks of waterborne typhoid. Unlike cholera, people infected with non-typhoid type bacteria can carry it without any symptoms of the disease (Wenneras *et al.* 2004; Cabral 2010)

2.1.4. *Shigella*

Shigella is a rod-shaped, gram negative bacterium that is closely related to *Salmonella*. The diseases caused by these bacteria is called shigellosis. *Shigella* has been found to be one of the leading bacterial causes of diarrhoea worldwide. The total number of *Shigella* outbreak that happens throughout the world each year has been reported to be 164.7 million. Around 163.2 million cases occur in developing countries, with 1.1 million cases resulting in death. Children under 5 years account for 62% of all deaths (Wenneras *et al.* 2004; Emch 2008)

2.2. Traditional disinfection methods

Determining and controlling the microbiological quality of drinking water is one of the important stages in the disinfection process. A disinfection process will either minimize or remove completely the microbial contaminants in water. There are many traditional disinfection methods available, such, as chlorination, ultraviolet radiation, iodination, ozonation and chloramines; each possessing their unique advantages and disadvantages. Although these disinfection methods can effectively remove and control the bacterial contaminants to the desired levels in water, research in the past years has revealed the formation of harmful Dibutyl phthalate (DBP) (Krasner *et al.* 2006).

Chemical disinfectants such as chlorine and ozone can react with various constituents in water to form DBP, which are carcinogenic. One of the challenges in disinfection is that some bacteria have become more resistant to the available disinfectants and require an extremely high disinfectant dosage, leading to more formation of DBP (Krasner *et al.*, 2006).

Therefore, in order to overcome the limitations of the traditional disinfection methods, research is underway in developing alternative disinfection methods that enhance the reliability and robustness of disinfection while avoiding Dibutyl phthalate (DBP) formation (Li *et al.* 2008). Apart from DBP formation, some of these technologies are often costly, too dangerous

and time consuming. Moreover, it is not known whether they can solve the challenges posed by new emerging contaminants that are a result from industrial activity. The disinfection of bacteria is determined by (Richardson 2003a; 2003b; Richardson 2004):

- i) How susceptible the bacteria are to the disinfectant
- ii) The contact time between the bacteria and the disinfectant
- iii) The concentration of the disinfectant dosage

In order for a disinfection method to be effective, the selection of which method to use will depend on the source of the water. For instance, a water source with high levels of turbidity or suspended solids may not work effectively with ultraviolet radiation method as these materials may react or absorb the UV radiation and therefore reduce its disinfection performance. Turbidity has no health effects in bacteria contaminated water, but it can shield the bacteria and provide a medium for bacterial growth (National Drinking water Clearinghouse 2014). For a disinfectant to be effective in inhibiting bacterial growth, it requires an uptake by the bacteria and subsequent transportation to the target sites of the bacteria. The accumulation of the disinfectant in higher levels will cause internal destruction of the bacterial cell and eventually cause cell death. A summary of some of the traditional disinfectants is given below, outlining their advantages and limitations (National Drinking water Clearinghouse 2014).

2.2.1. Chlorine

For more than a century, chlorine or chlorine products have been used as the most common disinfectants of drinking water. It is highly soluble and may be used as a gas, solid or even in liquid form to disinfect water. It is easy to use, inexpensive and its dosage is controllable.

Chlorine gas, however, is highly toxic and can be dangerous when released into the atmosphere.

This limitation can be avoided by using chlorine in its solid form as calcium hypochlorite or in its liquid form as sodium hypochlorite. It is also cost effective and reliable, with properties that prevent regrowth of microorganisms (Ministry of Health of Russian Federation 2014). Chlorine is very effective in removing almost all bacterial contaminants, but it reacts with organic compounds in water forming THMs and haloacetic acids which are carcinogenic. The control of THMs is important in water treatment but adds another level of difficulty into the process. As a result, many water systems limit the use of chlorine as a disinfectant. Strict requirements for transportation and storage are a necessity as it poses health risks in case of leakage (National Drinking water Clearinghouse 2014; Ministry of Health of Russian Federation 2014; Common Methods of Water Disinfection 2014).

2.2.2. Ozone

Ozonation or ozone disinfection is often used in large industrial plants after at-least a secondary treatment. It has been widely used to control taste and odour in wastewater treatment. Ozone is an unstable gas that can destroy bacteria, and usually a secondary disinfectant like chlorine is required because ozone does not maintain an adequate residual in water. The primary process that ozone disinfects is through oxidation. It is more effective than chlorine in the inactivation of viruses, *Cryptosporidium* and *Giardia* (Solomon *et al.* 1998; National Drinking water Clearinghouse 2014).

An ozone system is relatively complex to operate and maintain as compared to chlorination. It is costly to use and extreme caution is needed when operating. In its gaseous state, ozone is hazardous (Solomon *et al.* 1998). Although this method requires short contact time and low dosages, it may not effectively inactivate all bacteria; hence it is often used after secondary treatment. The production of DBP such as carcinogenic bromate is a possibility (Solomon *et al.* 1998; National Drinking water Clearinghouse 2014; Common Methods of Water

Disinfection 2014). Like chlorine, iodine is available in liquid and solid form. It is recommended to be used for emergency purposes only and in limited quantities. Water disinfected with iodine is not recommended for people who are pregnant or have a thyroid disease. High operational costs for this method also limit its usage (Common Methods of Water Disinfection 2014).

2.2.3. Ultraviolet light (UV)

Ultraviolet (UV) light/radiation can be attractive as a primary disinfectant because it is readily available and requires short contact time. It is effective against bacteria and viruses but not parasitic cysts. When UV radiation penetrates the cell wall of bacteria, it disrupts its DNA structure and makes the cell unable to reproduce (Common Methods of Water Disinfection 2014; National Drinking water Clearinghouse 2014). As with ozone disinfection, a secondary method is often necessary to prevent regrowth of the bacteria (Common Methods of Water Disinfection 2014). Water with high concentration of iron, turbidity and suspended solids may not be applicable to UV disinfection. High operating costs also limits this method from being used.

2.3. Preparation methods for synthesis of metal oxides/ NPs

Metal oxides can adopt a large variety of structural geometries with an electronic structure that may exhibit metallic, semiconductor, or insulator characteristics, endowing them with diverse chemical and physical properties. Metal oxides are the most important functional materials used for transduction and chemical and biological sensing. Moreover, their unique and tuneable physical properties have made themselves excellent candidates for electronic and optoelectronic applications. Nanostructured metal oxides have been actively studied due to both scientific interests and potential applications (Salavati- Niasari *et al.* 2009).

A wide variety of nanoparticles have been synthesised by mechano-chemical processing, including Zinc sulfide (ZnS), Cadmium sulfide (CdS), Zirconium (ZrO_2), Lithium manganese oxide ($LiMn_2O_4$), Silicon dioxide (SiO_2), Cerium oxide (CeO_2) and Zinc oxide (ZnO) (Salavati- Niasari *et al.* 2009). Mechano-chemical processing is a novel method involving the mechanical activation of solid-state displacement. Mechano-chemical synthesis is particularly suitable for large-scale production because of its simple process and low cost. The precursor can be examined by simultaneous differential thermal analysis (DTA) and thermogravimetric analysis (TGA).

2.3.1. Sol-gel

The sol-gel method is a wet chemical technique which is largely used in material science for producing solid materials from small molecules. It is primarily used for the production of materials, typically metal oxides, starting from the chemical solution (which is the sol, short for solution), which acts as the precursor for the intended product (or gel). A typical sol-gel process involves the formation of a diphasic system containing both the liquid phase and the solid phase, where the liquid may need to be removed by sedimentation or centrifugation to allow the separation of the two phases to occur and only the intended product to remain (Brinker and Scherer 1990).

The removal of the liquid phase may need a drying process which is often accompanied by shrinkage. The final product after drying is often influenced by the drying process. This route can be used to obtain functional materials with tailored properties for specific applications. The sol-gel process is inexpensive and a low-temperature operation technique that usually allows for control of the product's chemical composition (Klein 1994; Corriu and Anh 2009). Some limitations such as difficulty in controlling porosity and weak bonding have prevented the sol-gel method to be used at its full capacity for large production (Olding *et al.* 2001).

2.3.2. Reverse micelles

The reverse micelle method is one of the promising wet chemistry synthesis techniques for the production of nanomaterials. This method entails the preparation of two separate microemulsions, involving two different reactants. Microemulsion is a thermodynamically stable dispersion of two immiscible fluids; where the mixture is stabilized by adding a surfactant. After mixing these microemulsions, nucleation occurs on the micelle edges as the water droplets inside them become supersaturated with reactants. Growth then occurs around this nucleation point, where successful collision occurs between the micelle with the arrival of more fed reactants via the intermicellar exchange (Eastoe *et al.* 2006). The method provides a favourable environment for controlling the chemical reaction parameters. As such, it is possible to control the reaction rate and it is therefore easy to produce nanoparticles with narrow size distributions (Bae *et al.* 2005).

The method is also promising to restrict the agglomeration of particles and maintains the size distribution of these materials. One of the most important aspects of this method is the control of the nanoparticle size. Besides the stirring time and reaction temperature, the type of surfactant and the concentration of the reagents used are also crucial. The reverse micelle method is inexpensive as compared to other physical methods (Kumar *et al.* 2010).

2.3.3. Chemical reduction

Chemical reduction synthesis of nanoparticles uses the metal salt of the metal of interest as the precursor. The precursor is usually mixed with an appropriate solvent medium in the presence of reducing agents. The main advantage of this method is the use of affordable equipment, which can also be tailored to suit the desired properties of the intended applications. Depending

on the approach of the method, stabilizers play a role in this method controlling the size and dispersion of the nanoparticles (Guzman *et al.* 2009; Kheybari *et al.* 2010).

2.3.4. Microwave-assisted synthesis

While the preparation of nanoparticles and their composites is still largely based on conventional methods, many of these methods typically involve a lot of steps which can take long hours or even days. Moreover, some of these methods often lack good control of particle size, uniform particle distribution and large amounts of materials and energy are used. Only few reports provide simple, efficient routes for uniform dispersion and strong attachment of nanoparticles (Kheiralla *et al.* 2014).

Microwave-assisted methods have been widely applied in chemical reactions in the organic and medicinal community and have also gained momentum in polymer synthesis, material sciences and nanoscience. Research has shown the method to be advantageous over conventional methods (Nuchter *et al.* 2004). By conventional methods, the vessel is heated and this then transfers heat by convection. This is comparatively slow and inefficient for transferring heat to the system, since it depends on the thermal conductivity of the various materials that must be penetrated and results in the temperature of the reaction vessel being higher than that of the reaction mixture (Kappe 2004).

In contrast, microwave heating is more efficient in terms of the energy used and produces higher temperature homogeneity and is considerably more rapid than conventional heat sources. Microwave heating is the transfer of electromagnetic energy into thermal energy and is energy conversion rather than heat transfer. Microwave energy is similar to visible light, infrared irradiation and UV irradiation and is delivered directly to the material through a

molecular interaction with the electromagnetic field (Gedye *et al.* 1986; Kappe 2009). Since microwaves can penetrate the material and supply energy, heat can be generated throughout the volume of the material resulting in volumetric heating (Das *et al.* 2009). Additionally, the method has shown to reduce reaction time, increase product yield, generates small and narrow particle size distribution and high purity materials with enhanced physicochemical properties. Therefore, the use of microwave-assisted method in the preparation of nanoparticles and their composites offers advantages over the conventional methods (Miyawaki *et al.* 2006; Li *et al.* 2007).

2.4. Characterisation methods

The nanoparticles are characterised by UV–visible spectroscopy, Fourier Infrared Spectroscopy (FTIR), Transmission Electron Microscopy (TEM) and Scanning Electron Microscopy (SEM). In this research project, the synthesis of Co_3O_4 and ZnO nanoparticles by mechano-chemical processing will be investigated.

2.4.1. UV- Vis Spectroscopy

UV –visible spectra for synthesized nanoparticles shows the characteristic surface plasmon resonance (SPR) band which indicates crystalline spherical nature the NPs. The increase in intensity of UV absorption spectra indicates increase in the number of synthesised nanoparticles with increasing concentration as well (Rao 2010). The incident light acts as a catalyst which initiates the reduction process by breaking ionic bonds of metal NPs, there by creation of free moving ions. Light irradiation reduction of the nanoparticles will change the optical properties of colloidal solution, when the concentration of synthesised NP is changed, which can be related to the size and shape of the reduced nanoparticles (Shivananda *et al.* 2016). For the higher concentration, the intensity of the absorption peak is decreased and the

peak is shifted. The peak shift may be attributed to the change in particle size, this is confirmed by TEM analysis (Navale *et al.* 2015).

2.4.2. Fourier Infrared Spectroscopy (FTIR)

Fourier Infrared Spectroscopy (FTIR) is a method where IR radiation is passed through the sample. Some of the infrared radiation is passed through the sample and some of the infrared radiation is absorbed by the sample. The resulting spectrum represents the molecular absorption and transmission, creating a molecular footprint of the sample. The analysis is used to determine the chemical functional groups in the sample. Different functional groups absorb characteristics of IR radiation and is an important tool for structural elucidation and compound identification (Stuart 2005; Raliya *et al.* 2014).

2.4.3. Scanning Electron Microscopy (SEM)

Scanning Electron Microscopy (SEM) is a powerful magnification tool that utilizes focused beams of electrons to obtain information. SEM is a type of electron microscope that images the sample surface by scanning with a high energy beam of electrons in a raster scan pattern. The high resolution, three dimensional images produced by SEM provide topographical, morphological and compositional information (Swapp 2012).

2.4.4 Transmission Electron Microscopy (TEM)

Transmission Electron Microscopy was used to obtain the size and morphology of the nanoparticles. Samples were dispersed in distilled water and sonicated. A drop of the sample was deposited onto a copper grid of TEM and observed under high magnification (300000) (Guzman *et al.* 2009).

2.5. Antibacterial activity of ZnO NPs

2.5.1 Penetration mechanism of NPs

NPs introduce reactive oxygen species (ROS) in bacteria by diffusion. ROS is a generic term for molecules and reactive intermediates that possess strong positive redox potential, and different types of NPs produce different types of ROS by reducing oxygen molecules. The four ROS types are the superoxide radical ($O_2^{\cdot-}$), the hydroxyl radical ($\cdot OH$), hydrogen peroxide (H_2O_2), and singlet oxygen (O_2), which exhibit different levels of dynamics and activity. Zinc oxide NPs can generate H_2O_2 and $\cdot OH$ but not $O_2^{\cdot-}$. The main causes of ROS production are restructuring, defect sites, and oxygen vacancies in the crystal. Oxidative stress is caused when there is an imbalance between production and clearance of ROS in a bacterial cell as shown in **Figure 2.1**, which damages the individual components of a cell (Mohammad *et al.* 2012).

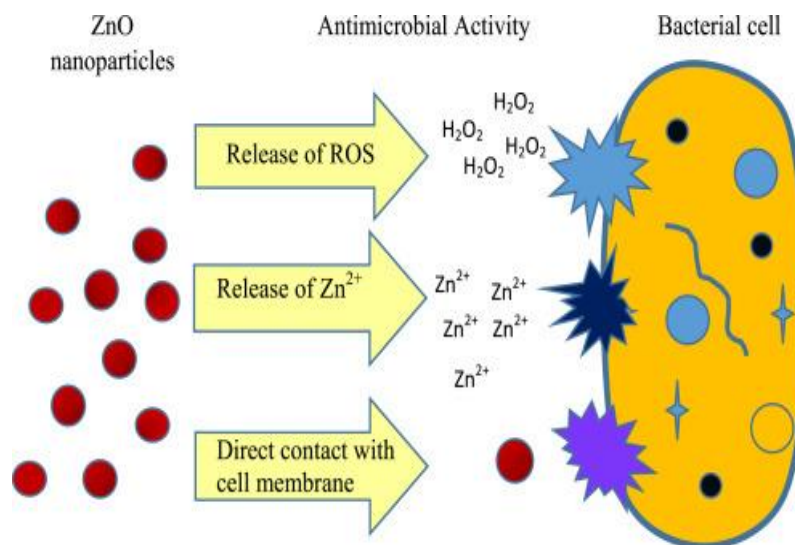


Figure 2.1: Antibacterial activity of ZnO NPs (Mohammad *et al.* 2012)

2.5.2. Antibacterial activity

The bacterial cell wall plays an important role in maintaining the bacterium's natural shape. The components of the cell membrane produce different adsorption pathways for NPs and Gram-positive and Gram-negative bacteria. Lipopolysaccharides (LPS) / lipoglycans is a

unique structure of the cell wall of Gram-negative bacteria that provides a negatively charged region that attracts NPs. On the other side, teichoic acid is only expressed in the cell wall of Gram-positive bacteria, so NPs are distributed along the molecular chain of phosphate, preventing their aggregation (Scott and Barnett 2006). The cell wall of Gram-positive bacteria has a thin layer of peptidoglycan as well as teichoic acid and abundant pores that allow foreign molecules to penetrate, resulting in cell membrane damage and cell death (**Figure 2.1**). In addition, compared with Gram-negative bacteria, Gram-positive bacteria have a high negative charge on the cell wall surface, which can attract NPs (Mohammad *et al.* 2012).

2.6. Methods used to assess antimicrobial activity

Nanotechnology is now creating a growing sense of excitement in the life sciences especially biomedical devices and Biotechnology. Antimicrobial capability of NPs allows them to be suitably employed in numerous household products such as textiles, food storage containers, home appliances and in medical devices (Prabhu, Divya and Yamuna 2010).

2.6.1. The disk diffusion method

The antibacterial activities of NPs can be carried out by disc diffusion method. In this method, nutrient agar medium plates were prepared, sterilized and solidified. After solidification bacterial cultures are normally swabbed on these plates. The sterile discs are dipped in nanoparticles/sample solutions and placed on the nutrient agar plate and kept for incubation at 37°C for 24 hours for bacteria and up to 7 days for fungal strains at room temperatures. Then zones of inhibition are measured and recorded. The presence of inhibition zones clearly indicate the antibacterial effect of the NP or NP composite (Cruickshank 1968).

2.6.2. Minimal inhibitory concentration (MIC)

Minimal inhibitory concentration (MIC) is used to test for antimicrobial activities of nanoparticles against test organisms. In this procedure, the dispersion of sample/ nanoparticles

are diluted in a 96 well microtiter plate by culture medium (Mueller Hinton broth) in geometric progression, from 2 to 2048 times. The concentrations of the samples in the dispersion sometimes range from 54 mg/l to 0.05 mg/l. After the dilution samples, a standard amount of test organism is being inoculated onto the microtiter plate, so that inoculum density in the wells will be 10^6 CFU/ml. The microtiter plates are incubated at 37°C, for 24 hrs. MIC is recorded as the lowest concentration of the agent inhibiting the visible growth microorganisms (Panacek *et al.* 2009).

2.7. Advanced NPs for disinfection purposes and their composites

2.7.1. Zinc nanoparticles

In order to demonstrate the antibacterial mechanism of the ZnO NPs, two methods were applied namely photocatalytic and Globally Harmonised System (GSH) oxidation protocol to measure the superoxide anion production. Normally, oxidative stress may come from nanomaterials itself and through disturbing microbial processes or oxidising vital cellular structure or components without (ROS) production *ie.* Reactive oxygen species (ROS) independent oxidative stress (Zhang *et al.* 2010; Zhang *et al.* 2014).

TiO₂ radiated with UV light was used as a positive control to validate the tests and along ZnO NPs (without radiating with UV light) as a negative control. It was found that ZnO NPs have the property to generate ROS in the presence of UV light; it could show significant antimicrobial activity in the presence of UV light because of ROS generation in the medium. After the 2, 4 and 6h incubation in UV radiation ZnO NPs have shown ascending levels of absorbance. The *in vitro* GSH oxidation protocol was carried further to figure out the second possible mechanism, as GSH is an antioxidant to bacteria, fungi and plants (Navale *et al.* 2015).

Those experiments proved that the antimicrobial activity of ZnO nanoparticles is dependent on the size of the nanoparticles and was mainly due to the particulate ZnO as the release of free

Zn²⁺ ions and Reactive Oxygen Species (ROS) from ZnO colloidal solution that was in the experiment. Those results were consistent with the earlier report of ZnO NPs with spherical shapes and 15-20 nm size (Krishna, Ranjit and Adhar 2011)

The potential applications of ZnO NPs in medical fields was realised, to get a better understanding of the antimicrobial toxicity mechanism. The possibility of superoxide anion induced by ROS production was evaluated by UV-mediated photocatalytic experiments, and *in vitro* Globally Harmonised System (GSH) (g-L-glutamyl-L-cysteinylglycine) oxidation methods. The study results suggested that the ZnO NPs and their photo catalytic properties contribute greatly to their antimicrobial activity with membrane and oxidation stress (Navale *et al.* 2015).

In conclusion, those results suggested that the ZnO NPs have greater efficacy in inhibiting the growth of *S. aureus* compared to the *S. typhimurium* and its inhibitory effects increase as the concentrations of ZnO NPs were increased. The MIC for *S. aureus* and *S. typhimurium* was 40 µg/mL. In case of *S. typhimurium* and *Aspergillus* the concentration of 80 to 100 mg/ mL were more enough to significantly control their growth which was demonstrated by weighing the fungal biomass. The antimicrobial mechanisms of the ZnO NPs, suggested that oxidation capacity of NPs toward GSH oxidation stress were responsible for antimicrobial behaviour of ZnO NPs. The results of *S. typhimurium*, and fungi *A. flavus* and *A. fumigates* suggest that ZnO nanoparticles are not only useful as an effective fungicide in agricultural and food packaging applications but also to control the growth of pathogenic bacteria (Navale *et al.* 2015).

The scope of ZnO nanoparticles has been a keen area of interest for biologists due to their distinct activity, which has opened new frontiers to biological sciences (Allaverdiyew *et al.* 2011). ZnO in its nanoscale form has a strong toxicity towards a wide range of microorganisms including bacteria (Huang *et al.* 2008; Abdelhay *et al.* 2012), fungi (He *et al.* 2011), fish (Lin

et al. 2011), algae (Wong *et al.* 2010) and plants (Lin & Xing 2008). The antibacterial activities of ZnO against pathogenic bacteria such as *E. coli* and *S. aureus* strains are well documented (Navale *et al.* 2015).

Previous studies on the antibacterial behavior of Zinc NPs have shown that the morphology and oxidative stress play important roles in the antibacterial activity (Sourabh *et al.* 2014; Krishna, Ranjit and Adhar 2011). Due to the quite similar nanosized structure of ZnO NPs to other oxide nanoparticles, it is necessary to examine oxidative stress in order to explore how ZnO NPs kill the microorganisms including bacteria and fungi.

2.7.2. Cobalt nanoparticles

As a nanoparticle, cobalt-based nanoparticles may be produced as cobalt oxide, organic metal compounds or biopolymers. Cobalt nanoparticles have been investigated for use in cancer therapy and anaerobic waste water treatment (Sadjadi *et al.* 2006). A large number of reports on the antibacterial properties of cobalt complexes have appeared in the literature, with Co(II) complexes being the most studied, presumably due to their aqueous stability, availability, and ease of synthesis. However, Kuo *et al.* (2006), reported that Cobalt nanoparticles have no antibacterial activity towards *S. aureus* or the Gram-negative bacteria *E. coli* and *Enterobacter faecalis*. Cobalt exposure is known to lead to various lung diseases, including interstitial pneumonitis, fibrosis, asthma and cancer. This raises the challenge of toxicity when using Cobalt in the treatment of drinking water. However, toxicity studies will be required to address this issue in water treatment (Lison *et al.* 1996; Kuo *et al.* 2006).

Reports on the antibacterial properties of cobalt (III) complexes frequently emphasise the increased effectiveness of cobalt ion coordination to a particular ligand when compared to the free ligand itself. Complex 9, containing a new hybrid amine-imine-oxime ligand derived from

the condensation reaction of diacetylmonoxime with benzidine, was shown to be effective against *Bacillus subtilis* (Kaya *et al.* 2008).

In a study by Kaya *et al.* (2008), cobalt complexes was less effective than the control antibiotics tetracycline and kanamycin (using μg of antibiotic per unit volume). Complex 9 is neutral due to the presence of one deprotonated oxime N-OH group and the oxidation state was assigned using magnetic moment measurements and absorption spectra. The related vic-oxime complexes 10 were described by the same authors (Canpolat and Kaya 2004). Complexes 10a–f all showed antibacterial activity towards *Enterobacter aeruginosa*, *E. coli*, *S. aureus*, and *B. subtilis* but were all less effective than the commonly used macrolide antibiotic azithromycin.

Cobalt nanomaterials were applied as a bactericidal agent to control waterborne bacterial pathogens. Cobalt doping on zinc oxide and exposure of sunlight enhanced the antibacterial activity against the selected waterborne bacterial isolate at 50 μg concentration. Interestingly, most effective bactericidal results were found against *Escherichia coli* and *Vibrio cholerae* (Ovmes *et al.* 2015).

2.7.3. Cobalt doped Zinc oxide nanoparticles

The most often obtained forms of $\text{Zn}_{1-x}\text{Co}_x\text{O}$ nanomaterials are: nanoparticles (NPs), nanorods, nanowires, nanoflowers, core-shells, and thin films (Kaushik *et al.* 2013, Nair *et al.* 2011). $\text{Zn}_{1-x}\text{Co}_x\text{O}$ nanomaterials can be obtained by such methods as, sol-gel (Shi *et al.* 2010, Kaushik *et al.* 2013), precipitation (Fabbiyola *et al.* 2015), calcination (Hadzic *et al.* 2012) vaporisation-condensation (Martinez *et al.* 2005), pulsed-laser deposition (Ivill *et al.* 2008), hydrothermal synthesis (Hadzic *et al.* 2012), solvothermal synthesis (Jayakumar, Sudarson and Tyagi 2015), combustion (Basith *et al.* 2014), and microemulsion (Li *et al.* 2016). Some of the most interesting methods of $\text{Zn}_{1-x}\text{Co}_x\text{O}$ NPs and ZnO NPs syntheses are microwave-assisted syntheses.

The dynamic development of the broadly understood microwave heating technology and the new design solutions of microwave reactors have contributed to the increased popularity of the microwave solvothermal synthesis (MSS) (Wojnarowics *et al.* 2016) and the microwave hydrothermal synthesis (MHS) methods. In the case of the synthesis of doped ZnO NPs, it must be emphasised that microwave methods ensure 100% purity of reaction conditions thanks to the course of synthesis in a reaction chamber formed in a chemically inert material, *eg.* Teflon[®]. Synthesis reaction purity is necessary for obtaining doped ZnO NPs with a repeatable chemical composition. Doped ZnO NPs obtained by microwave methods, *eg.* MSS, are characterised by high purity (contactless heating method), homogeneity, narrow particle size distribution, repeatability, and a low degree of agglomeration and aggregation (Wojnarowics *et al.* 2016).

According to Wojnarowics *et al.* (2016); Shi *et al.* (2010); Kaushik *et al.* (2013) and Nair *et al.* (2011), the literature review reveals that the magnetic and optical properties of the obtained Zn_{1-x}Co_xO NPs result from the employed synthesis method and sample preparation process. Despite the numerous publications, the topic of the syntheses and properties of Zn_{1-x}Co_xO NPs still remains quite controversial. The majority of papers argue that the ferromagnetic properties of the obtained Zn_{1-x}Co_xO samples result exclusively from intrusions of foreign phases, not from the presence of the Co²⁺ dopant itself.

Skilful selection of the synthesis method and sample preparation process of Zn_{1-x}Co_xO is extremely important since it permits avoiding the formation of foreign phases, *eg.* cobalt oxides (CoO, Co₂O₃, CoO(OH), Co₃O₄ , metallic cobalt (Wojnarowics *et al.* 2015; Park *et al.* 2004) and spinel zinc cobaltite (ZnCo₂O₄) (Kuryliszyn- Kudelska *et al.* 2013).

The leitmotif in the majority of publications is the examination of the impact of the $Zn_{1-x}Co_xO$ synthesis method on the properties of the obtained samples, while the issue of precise control of $Zn_{1-x}Co_xO$ NPs size is discussed sporadically. One of the easiest and most popular methods of changing the $Zn_{1-x}Co_xO$ NPs size is sample soaking, *eg.* in a chamber furnace, where the high temperature causes particle growth (Nair *et al.* 2011; Fabbiyola *et al.* 2015).

The application of microwave synthesis contributes to the change of $Zn_{1-x}Co_xO$ NPs properties, not only as a result of the change of their size but also through the precipitation of foreign phases. The soaking of $Zn_{1-x}Co_xO$ samples in an oxidising atmosphere usually causes the oxidation of Co^{2+} to Co^{3+} and the formation of various cobalt oxides (Shi *et al.* 2007) and spinel zinc cobaltite. The soaking in a reducing atmosphere, in turn, causes the reduction of Co^{2+} ions to metallic Co. $Zn_{1-x}Co_xO$ NPs prepared by this method are characterised by a compact heterogeneous structure (Kuryliszyn- Kudelska *et al.* 2013).

Another method that permits controlling the $Zn_{1-x}Co_xO$ NPs size by changing the synthesis duration and temperature is the hydrothermal method (Annesh *et al.* 2010). The mechanism of $Zn_{1-x}Co_xO$ particle growth is explained by the phenomenon of recrystallisation. However, the hydrothermal synthesis of $Zn_{1-x}Co_xO$ NPs may lead to formation of foreign phases, *eg.* Co_3O_4 and $ZnCo_2O_4$ (Kuryliszyn- Kudelska *et al.* 2013) while synthesis products are usually heterogeneous (Xu and Cao 2010). One of the most interesting and promising methods of obtaining $Zn_{1-x}Co_xO$ NPs is the solvothermal method, where the size, morphology, and magnetic properties depend on the type of the organic solvent used (Jayakumar *et al.* 2015)

Wojnarowics *et al.* (2015) have proven the usefulness of the MSS in obtaining homogeneous $Zn_{1-x}Co_xO$ NPs, in which no precipitated foreign phases were detected. The zinc acetate, cobalt acetate, and ethylene glycol (EG) were used as reagents. The organic solvent selected (EG), had reducing properties, thanks to which it prevented the oxidation of Co^{2+} to Co^{3+} during the synthesis. At the same time, it is a too weak reducing agent to reduce Co^{2+} to metallic Co. It must be emphasised that the MSS method also has great potential for obtaining ZnO NPs. The MSS of ZnO NPs developed by Wojnarowics *et al.* (2016), permits controlling the NPs size within the range of 15 nm to 120 nm.

2.8. Water toxicity tests

Even though most NPs are known to have antimicrobial activity, some of them are toxic to the surrounding environment. Therefore, a toxicity test is of vital importance when dealing with NPs in water analysis. The measure of toxicity is an integral view of the sum of all interacting components in the sample. The purpose of regulatory toxicity testing is to produce baseline data for environmental hazard and risk assessment of chemicals, to be used in regulating the discharge of wastewater treatment systems (Tyagi *et al.* 2007).

Bioassay has been extensively used to document toxicity of surface water and evaluate the potential toxicity of discharges into these waters (Blinova 2000). Numerous studies have been made to understand the toxic effects of waste effluents on fish, but relatively little attention has been paid to their adverse effects on plankton. In view of the importance of cladocerans as an important link in the food chain in aquatic ecosystem, the recent toxicity studies use *Daphnia magna* Straus. It is highly sensitive to toxic substances, has short generation time, multiplies very rapidly, easily acclimatizes in laboratory condition, is cultured in a small space and can be measured in a relatively short period (APHA 1998; GSM 1989).

The use of *Daphnia magna* in toxicology is accepted in several countries to monitor wastewater treatment systems, to establish quality criteria, to determine permissible concentrations of pollutants, limits of impurity in water from natural effluents, and to determine the efficacy of a good sanitation method.

In this study, a modern review of Zinc Oxide and Cobalt oxide nanostructure, its unique characteristics at nanoscale level and the properties are presented through an analytical process and antimicrobial studies. Their behavior at nanoscale is explored and its toxicity in aquatic environment is presented. Finally, this review was concluded with many future scopes and enhancement.

If these nanoparticles can show an ability to inhibit the growth of selected water pathogens, they can be used to treat contaminated water and waste water. Consequently the mortality rate that is caused by consumption of untreated water containing *V. cholerae*, *Salmonella etc.* can be reduced annually. It is estimated that 10% of diseases worldwide can be prevented by improving the water supply, sanitation, hygiene and management of water sources (WHO 2013). These nanoparticles can also than be used to produce inorganic antibiotics and antimicrobial substances.

CHAPTER 3

RESEARCH METHODOLOGY

This chapter provides a detailed description of the experimental procedures of the studies carried out. It includes the description of the modification of the nanomaterials and the description of the different techniques used to characterise the materials and the procedure used to carry out the antimicrobial studies.

3.1 Reagents and chemicals

All chemicals and reagents, unless otherwise indicated, were obtained from suppliers and used without further purification.

Zinc acetate (99 %) + urea (99 %), KOH, ethanol, Cobalt nitrate hexahydrate, Ammonium carbonate, oxalic acid, zinc acetate (99%), urea (99%), zinc sulphate, diethyl glycerol, Co (NO)₂ · 6H₂O, NH₄ HCO₂ (2: 5), cobalt acetate, Zn (Ac)₂ · 2H₂O (99, 9 %, Sigma) and cobalt acetate tetrahydrate, Co (Ac)₂ · 4H₂O (99, 9 %) were purchased from Sigma Aldrich, South Africa.

3.2 Synthesis of nanoparticles – Experimental procedure

Synthesis and characterization of the NPS were carried out in the Chemistry Department, Vaal University of Technology, South Africa.

3.2.1 Urea based synthesis of ZnO nanoparticles

Starting materials: Zinc acetate (99 %) + urea (99 %)

The calculated amounts of their grams were measured, Zn (ac) 10.975 g and Urea 3.006 g. They were dissolved in 50 ml of deionised water under constant agitation, using 500 rpm. The KOH (3 mol/L) was added until pH reached 12. The solution was stirred at room temperature

for 15 min. The solution was heated through microwave hydrothermal synthesis (MHS) at 100° C for 4 hours. It was cooled at room temperature and centrifuged. The resultant white precipitate was washed with water and ethanol twice (Marinho *et al.* 2012). Then white product was dried at 60 °C for 5 hours. Ratios (Zn acetate: Urea) 1:1, 1:2, 2:1 and 1:4.

3.2.2 Synthesis of Co₃O₄ nanoparticles using mechanochemical synthesis

Starting materials: Cobalt nitrate hexahydrate + Ammonium carbonate (2:5)

A 5 g of Co (NO₃)₂ · 6H₂O and calculated amounts NH₄ HCO₂ were dissolved in 150 ml of deionised water and mixed under constant agitator for 90 min. Solution was centrifuged for 5 min. The precipitate was washed twice with deionized water. Final product of nanoparticles was dried at 100 °C for 2 hours. The samples were put in a muffle furnace and calcined for 2 hours (Yang *et al.* 2003). Nanoparticles were prepared using the following ratios [Co (NO)₂ · 6H₂O : NH₄ HCO₂ COO.NH₄.] 1:1, 1:2, 2:1, and 1:4.

3.2.3 Synthesis of Co. doped ZnO nanoparticles

The starting material: zinc acetate dihydrate, Zn (Ac)₂ · 2H₂O (99, 9 %, Sigma) and cobalt acetate tetrahydrate, Co (Ac)₂ · 4H₂O (99, 9 %, Sigma).

The Zn (Ac)₂ · 2H₂O (2.195 g) and Co (Ac)₂ · 4H₂O were dissolved in 50 ml of methanol under vigorous stirring at room temperature then ultrasonicated for 10 min. The solution was heated at 65°C under reflux for 2 h. The precipitates were collected and washed with absolute ethanol several times to remove excess reagents possibly remaining in the final products. Precipitates were then dried at 60°C for 2 h. Then a precipitate was calcined at 300°C for 1 h. A blue solid was obtained from pink cobalt ion solution (Hammad *et al.* 2012).

3.3 Characterisation of the synthesised nanoparticles

These are physical characterisation techniques which includes techniques that explain the size, charge, shape and composition of synthesised materials. The theory and principle of these techniques are detailed in this subsection.

3.3.1 Fourier Transform Infra-Red spectroscopy (FTIR)

Infrared spectroscopy analysis was carried out using a Fourier Transform spectroscope (Perkin Elmer spectrum 400). A sample was placed on a sample holder and clamped tight. Measurements were carried out in the range of 400 to 4000 cm^{-1} at resolution of 4 cm^{-1} (Radu *et al.* 2012; Kumar and Sangwan 2011).

3.3.2 UV-Vis spectroscopy

The optical absorption spectrum of nanoparticles was obtained using a UV-Vis spectrophotometer (T80+ UV-Vis spectrometer). One mg of ZnO, Co_3O_4 and Co- ZnO nanoparticle samples were dispersed in 1.5 ml of Toluene reagent and sonicated for 30 min. The spectrum was recorded in the range of 200 to 600 nm (Hebeish, Shaheen & Naggar 2016).

3.3.3 Scanning Electron Microscopy (SEM)

During SEM analysis, samples were loaded on a movable stage under the vacuum. The sample surfaces were scanned by moving the electron- beam coils. The beam has enabled the information about defined area of the sample. It showed detailed images at much high magnifications (up to 300000). Images were created without light waves (black and white) (Joshi *et al.* 2008; Alias, Ismail and Mohamad 2010).

3.3.4 Transmission Electron Microscopy (TEM)

Transmission Electron Microscopy was used to obtain the size and morphology of the nanoparticles. Samples were dispersed in distilled water and sonicated. A drop of the sample

was deposited onto a copper grid of TEM and observed under high magnification (300000) (Guzman *et al.* 2009).

3.4 Antibacterial Activity

3.4.1 Prerequisites

Microorganisms

Bacterial strains: *Salmonella enterica*, *Escherichia coli*, *Shigella sonnei* and *Staphylococcus aureus*, yeast and mould, *Candida albicans* and *Aspergillus niger* were obtained from VUT research laboratory. The antimicrobial activity experiments were carried out in the Department of Biotechnology, Faculty of Applied and Computer Science at Vaal University of Technology, South Africa. Bacterial strains in Table 1 below were subcultured on Nutrient agar plates and incubated for 24 h. *Candida albicans* and *Aspergillus niger* were subcultured in potato dextrose agar (PDA) for 48 h. Then organisms were inoculated in Mueller Hinton broth and incubated for 24 hours and serially diluted up to 10^5 (colony forming unit) CFU.

Nanoparticles

The working concentration for the NPs was 2 mg/ml in all ratios of the NPs and they were dissolved in distilled water.

Neomycin antibiotic

This positive control was dissolved in water at a concentration of 2 mg/ml.

Resazurin dye

The dye was used at 0.02 % concentration and was dissolved in distilled water. Everything was stored was kept in refrigerator after preparation.

3.4.2 Agar deep well diffusion

The antibacterial activities of NPs were carried out by well diffusion method. Mueller Hinton agar medium was prepared using distilled and autoclaved for 15 min. Medium was poured into plates and solidified. After solidification, bacterial cultures were swabbed on these plates. Four wells in each plate were created using sterile tips. At the center there was a well for positive control (neomycin). The working concentration of the neomycin was 2 mg/ ml. The working concentration for ZnO, Co₃O₄ and Co-doped ZnO NPs started at 2 mg/ ml, but it was increased further to 30 mg/ml for better results. A volume of 20 µl was loaded on the Mueller Hinton agar wells from all NPs and their prepared ratios. Plates were incubated at 37°C for 24 hrs (Savithamma *et al.* 2011). Zones of inhibition for control, ZnO, Co₃O₄ and Co-doped ZnO NPs were measured.

Antifungal activity: Potato dextrose agar plates were prepared, sterilized and solidified. After solidification, fungal cultures were swabbed on these plates. Wells were created in each plate. A volume of 20 µl was loaded on the Mueller Hinton agar wells from all NPs and their prepared ratios. The final working concentration was also 30 mg/ ml. The plates were kept for incubation for 72 h at room temperature. After 72 h, zones of inhibition were measured.

3.4.2 Minimum inhibitory concentration assay (MIC)

MIC was determined by broth microdilution technique. The 96 well plates were labeled from A to H and 1 to 12. A volume of 100 µl Mueller Hinton broth was added in all the wells. In wells 1- 6, 100µl of NPs was added (1- 3 wells Co₃O₄ and 4- 6 ZnO NPs). The prepared standard concentration NPs were serially diluted from A down to H. In wells 7 and 8 (-ve), there was no antibiotic nor NPs added. Neomycin antibiotic (+ve control) was added in wells 9- 10 and also diluted the same way with NPs. After the dilution, concentrations were as follows A 50 µg/ml, B 25 µg/ml, C 12.5 µg/ml, D 6.25 µg/ml, E 3.125 µg/ml, F 1.563 µg/ml, G 0.781 µg/ml, and H 0.391 µg/ml.

A volume of 70 µl of broth was added from 1- 10 down to H and 120 µl of broth was added in 11 and 12. That was done to make a single strength of 250 µl in each well. Then 50 µl of bacterial culture was added in all wells except in 11 and 12. These two wells act as positive control that confirms the sterility of the broth. Later 30 µl of resazurin dye was added prior to incubation and plates were incubated overnight at 37°C. Resazurin dye is blue in color when there is no growth and pink in color when microorganisms grow.

The strains were grown and maintained on Nutrient Agar at 37⁰ C for 24 hours and subcultured weekly. Stock cultures were stored at 4⁰C. Below, Table 3.1, is a list of the microorganisms that were used for antimicrobial studies.

Table 3.1. Waterborne pathogens

BACTERIA	GRAM STAIN	YEASTS	MOULDS
<i>Salmonella enterica</i>	Negative	<i>Candida albicans</i>	<i>Aspergillus niger</i>
<i>Escherichia coli</i>	Negative		
<i>Shigella sonnei</i>	Negative		
<i>Staphylococcus aureus</i>	Positive		

3.5 Toxicity test using *Daphnia magna* (Daphtox) kit

The kit was collected from Ambio Environmental laboratory at Vaal University of Technology

Preparation of standard water



Figure 3.1: Concentrated salts that are used to prepare standard water

Standard water was prepared by adding up four vials of concentrated salts from the kit, in a 2 L volumetric flask. A flask was filled up to 2 L mark by distilled water and aerated for 15 min.

Hatching of Ehippia

Aluminium foil was removed from a tube with Daphnia Ehippia. Contents of the tube with Ehippia was poured in the microsieve and rinsed thoroughly with tap water. Ehippia was transferred into a petri dish containing standard water and incubated for 72 h at 22°C under continuous illumination of 6 000 lux.

Preparation of the toxicant dilutions

The toxicants used were ZnO, Co₃O₄ and Co-doped ZnO NPs

C 1 = 0.5 mg/ ml, C 2 = 0.25 mg/ ml , C 3 = 0.125 mg/ ml, C 4 = 0.0625 mg/ ml and C 5 = 0.0313 mg/ ml



Figure 3.2: Apparatus for the dilution of nanoparticles using standard water

Five 100 ml volumetric flasks were labeled C1- C5 and filled with 50 ml standard water. Amount of 50 mg of NPs was weighed and added into the first flask (C 1). The solution was mixed for 1 min and flask was filled with standard water up to 100 ml mark. A two fold dilution was made by transferring 50 ml of the solution to C 2. Solution was mixed for a minute and the same dilution procedure was made to C 3, till final flask C 5 was done.

Filling of the test plate

After 72 h of incubation, the hatching of the *Daphnia magna* neonates was verified. In the test plate each well of the control row was filled with 10 ml of standard freshwater. Then 10 ml of respective toxicant concentrations were transferred into each well of the corresponding rows from C 5 to C1. The Spirulina suspension was added in a petri dish containing *Daphnia magna* neonates and the dish gently swirled and left for 2 h at room temperature, to allow neonates to feed and grow. For each test, 120 neonates were used. The transfer of *Daphnia* was as follows: 20 cells of *Daphnia magna* to the rinsing cup of the control, 20 cells of *Daphnia magna* to all rinsing cups of increasing concentrations of the toxicant using the Pasture pipette. Each diluted

concentration was tested 4 times including control raw using 5 cells *Daphnia magna* in each well. A piece of parafilm was put on the multiwell and plates were tightly covered. Plates were incubated at 22°C in darkness for 24 to 48 h.

Scoring of the results

The results were scored after 24 h and 48 h of incubation. The multiwell plate was put on the light table and the number of immobilized *Daphnia* cells were recorded.

CHAPTER 4

RESULTS AND DISCUSSION

4.1. INTRODUCTION

In this chapter, all the characterization of the materials with the different techniques (UV-Vis, FTIR, TEM and SEM) were discussed.

4.1.2 CHARACTERISATION RESULTS

4.2. SYNTHESISED NPs

4.2.1. ZnO NPS

The use of microwave heating (MH) crystallisation facilitates the direct preparation of pure oxide nanoparticles in less time with desired particle sizes and shapes from the control parameters such as solution pH, reaction temperature, reaction time, solute concentration and the type of solvent (Lee and Choi 2004). In the crystal growth process, first ZnO tiny crystalline nuclei were formed, and nanoparticles of this oxide were precipitated by an increase in pH due to NH_4^+ ions generated from NH_3 which resulted from urea decomposition when the temperature was rising. The NH_4^+ ion formation is controlled by ammonia in water, and the hydrolysis of urea leads to a rise in the pH. The urea hydrolysis progresses slowly, and the basic solution undergoes supersaturation of the zinc hydroxide species (Kakiuchi *et al.* 2006).

4.1.2. Co_3O_4 NPS

When preparing the Co_3O_4 NPs (Fig: 4.1 B) the reaction was observed very fast. The solution and precipitate was pink but turned grey/ black after being calcined (heated) at 300 °C. Figure

4.1B shows calcination of the Co_3O_4 precursor at 300°C using different ratios, resulted in the formation of the NP size.

4.1.3. Co-doped ZnO NPs

During the synthesis of Co-doped ZnO NPs the reaction and color change was observed very fast. All the dopant precipitates were light pink to pink, as the dopant percentage was increased. After being calcined at 300°C for 1 h, all the NPs became green.

4.2 UV-Visible spectroscopy

In UV-Visible spectroscopy, light is used to populate the unoccupied electronic states of the sample and transitions between the valence and conduction bands. The spectra were recorded in absorption mode and all samples were prepared by dissolving the nanoparticles in distilled water (Chandra and Kumar, 2012).

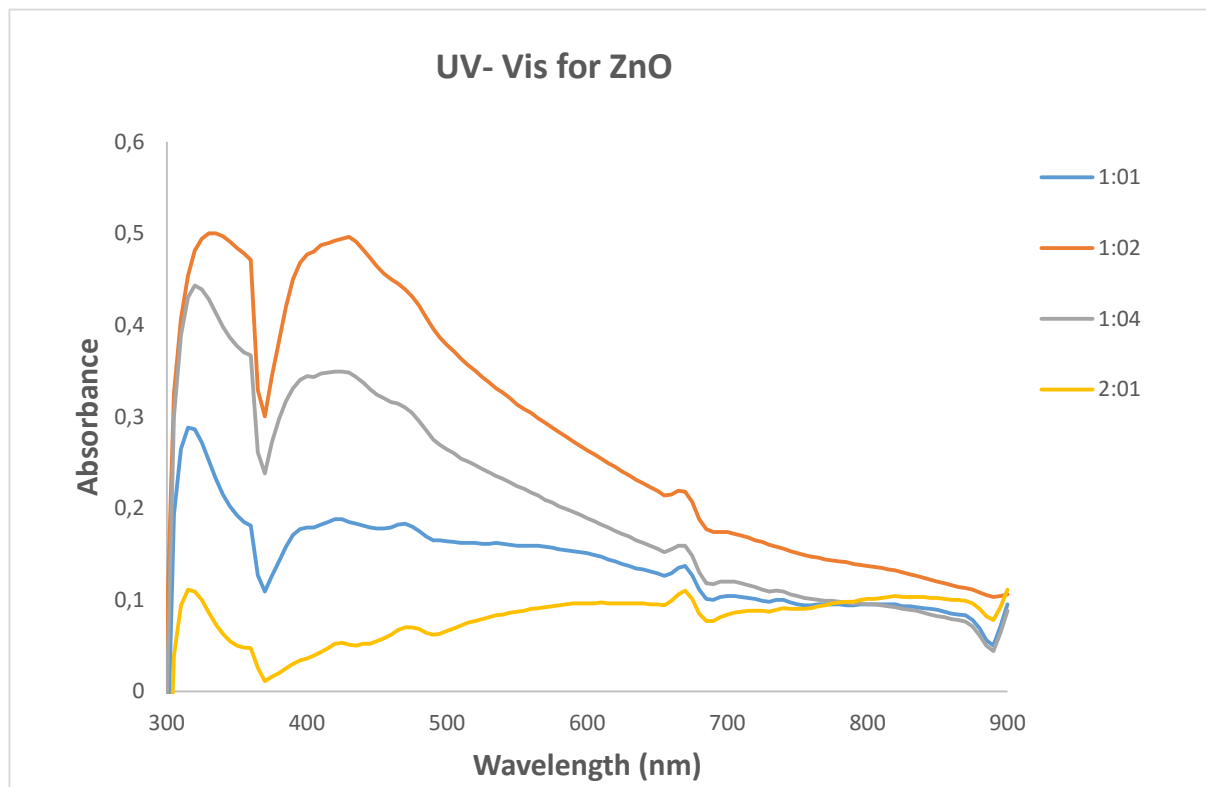


Figure 4.1: UV-Vis absorption spectrum recorded for ZnO

The absorption spectrum (**Figure 4.1**) of the white crystal ZnO colloids prepared by urea reduction showed a surface plasmon absorption band with a maximum of 320 and 450 nm indicating the presence of spherical or roughly spherical ZnO nanoparticles. The only difference between the samples is the absorbance. Sample ratio 2:1 has high absorbance as compared to the other samples. The sample has more molecules that interacted with light intensity of UV this increase the absorbance. The used mole ratio resulted in more bonds and more molecules to absorb the UV light (Guzman *et al.* 2009).

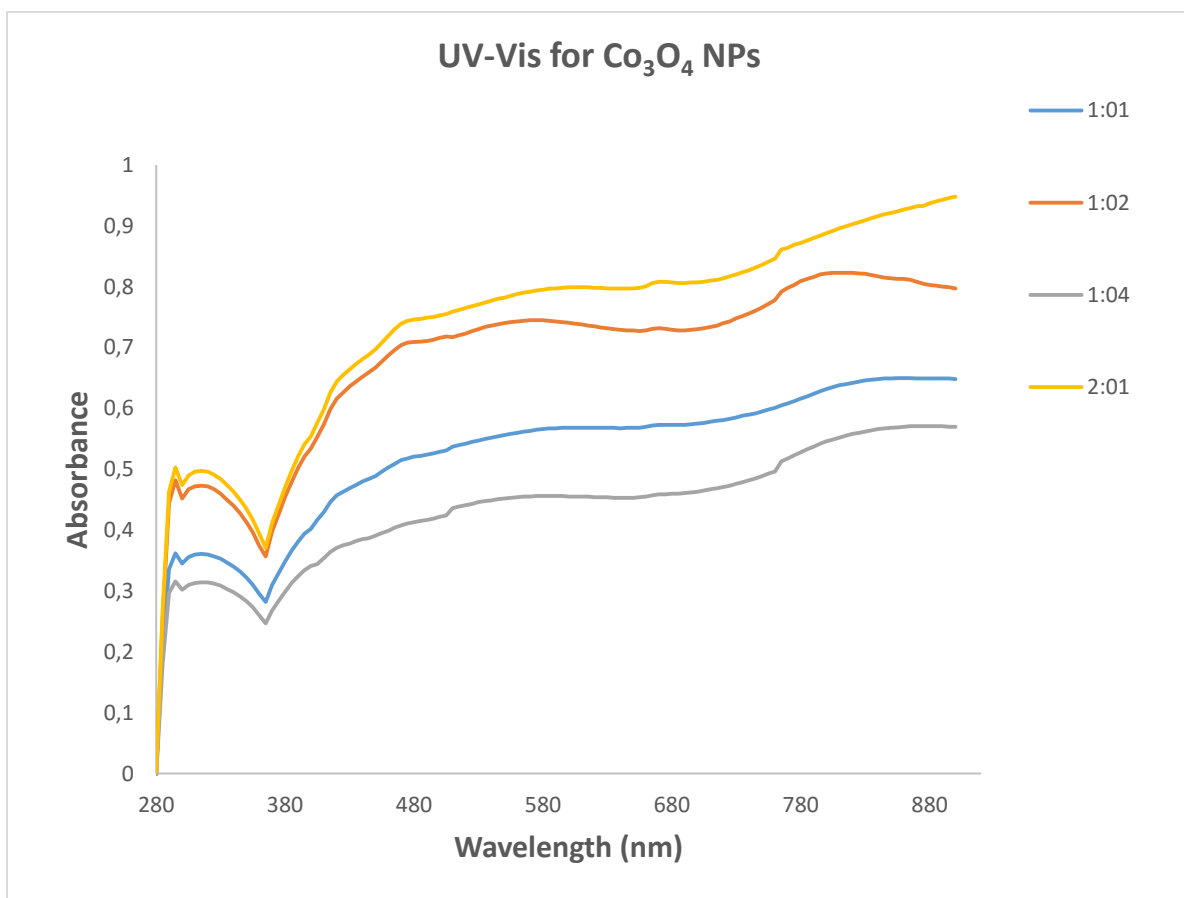


Figure 4.2: UV-Vis absorption spectrum recorded for Co₃O₄ NPs

An optical property of cobalt oxide nanoparticle was recorded with respect to high purity, and its crystallinity was confirmed with the help of UV-visible absorption spectra by observing an excitonic absorbance band at 300 nm with a tail extending towards a longer wavelength due to their quantum size effects as shown in **Figure 4.2**. The absorption peaks exhibit a slightly broad

peak due to the particle size. All the particles 1:1, 1:2, 1:4 and 2:1 showed the same peaks. The absorption band gaps are blue shifted to a high energy compare with bulk cobalt. The blue shift phenomenon of the absorption edge has been described to a decrease in particle size. It is well known in case of semiconductors that the band gap between the valence and conduction band increases as the size of the particles decreases in the nano-scale range. The magnitude of the shift depends on the size of the semiconductors material (Ather *et al.* 2012; Zhang and Xue 2002).

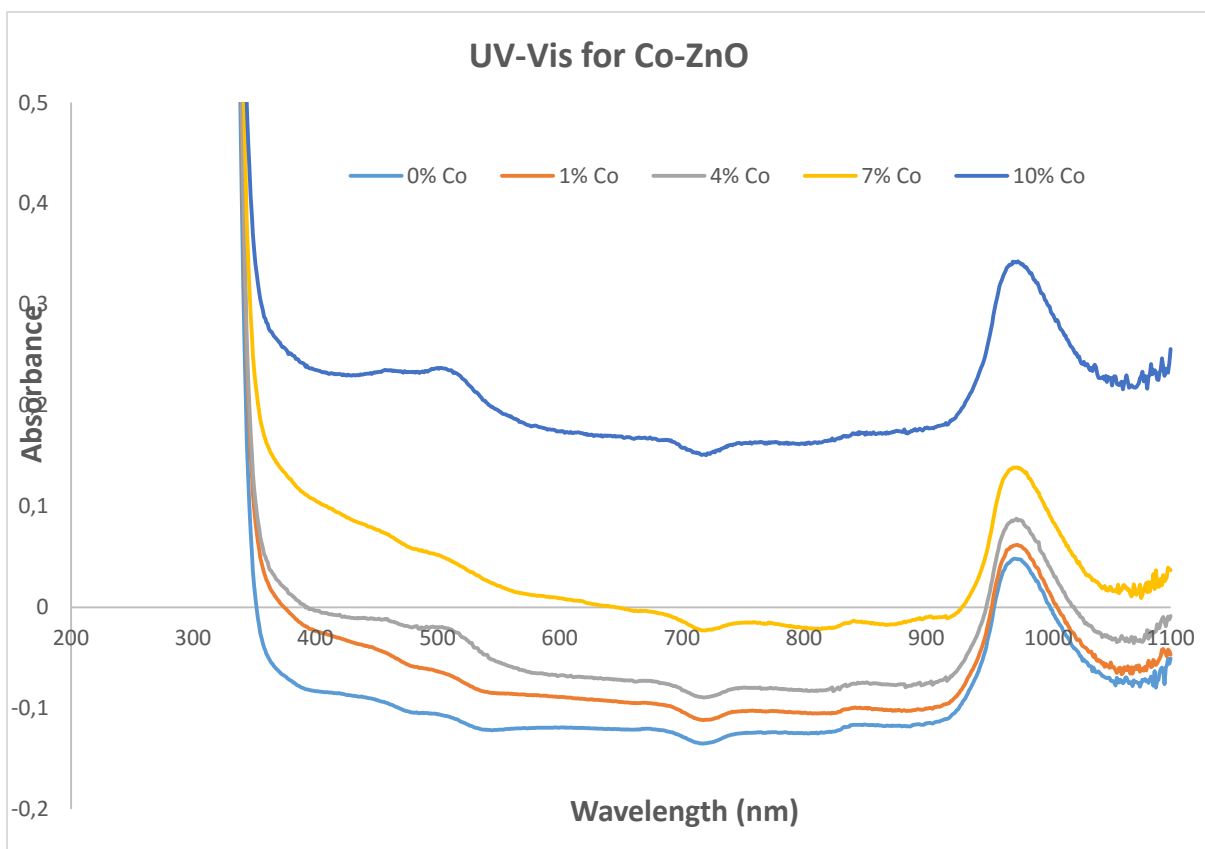


Figure 4.3: UV-Vis absorption spectrum recorded for Co–doped ZnO NPs

Figure 4.3 shows the UV-Vis spectrum of Co-ZnO particles with different doping concentration at room temperature. The change in absorption peak due to doping indicates a change in band structure. A blue shift is observed in the bandgap energy for the cobalt dopes samples compared to the undoped ZnO. The increase in the bandgap or blue shift is the

phenomenon that the Fermi levels merges into the conduction band with an increase in the concentration from 0 to 10% (Ather *et al.* 2012).

4.3 FTIR spectral analyses

The Fourier Transform Infrared (FTIR) spectra of ZnO, Co₃O₄ and Co-doped ZnO nanopowders were recorded in the range of 4000 – 500 cm⁻¹ using an Elmer FT-IR/ FT-NIR spectrometer (model 400).

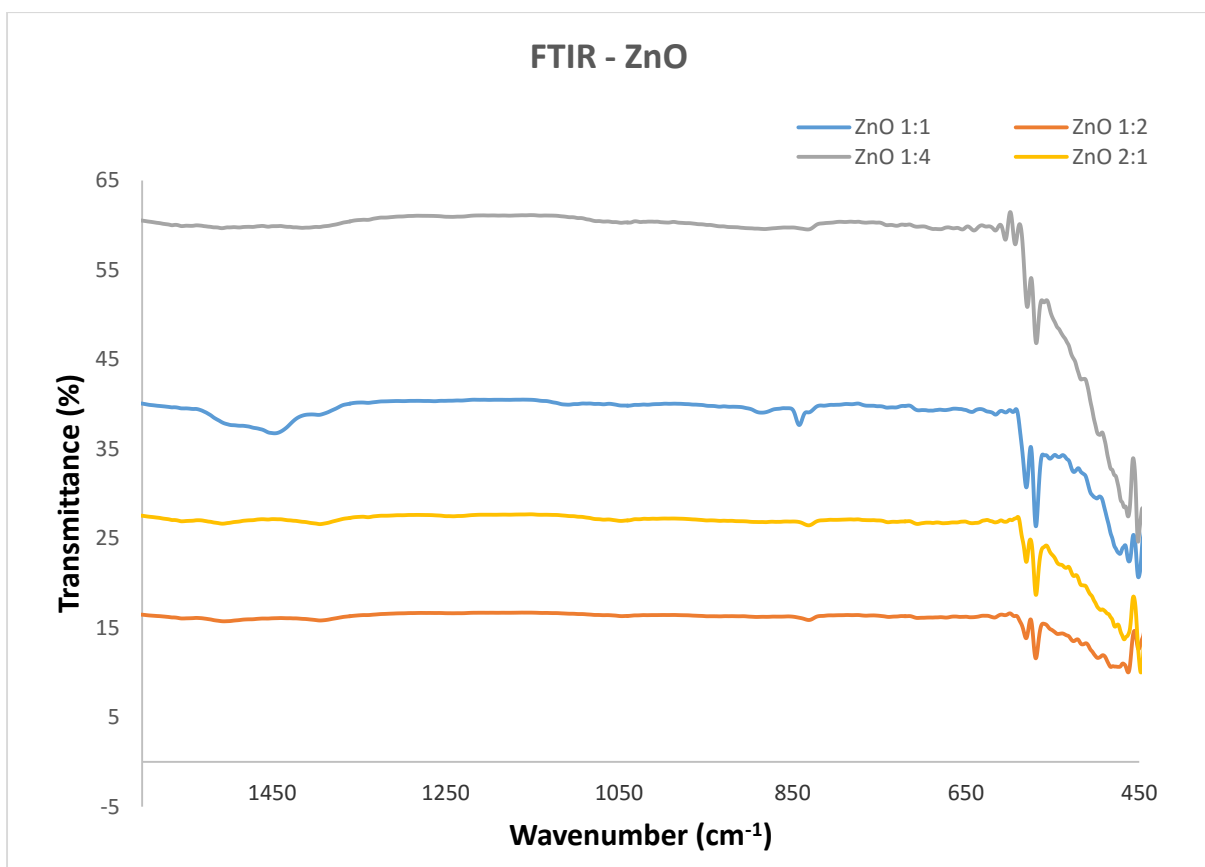


Figure 4.4: FTIR results for ZnO NPs at different ratios.

FT-IR spectra of synthesised zinc oxide with different mole ratios are shown in **Figure 4.4**. All the mole ratio samples shows similar absorption peaks. The spectrum shows absorption peaks below 600 cm⁻¹, which corresponds to the characteristics absorption of Zn-O in zinc

oxide The stretching band at 1423.54 cm^{-1} corresponds to carbonyl group (C=O) (Pal and Giri 2011).

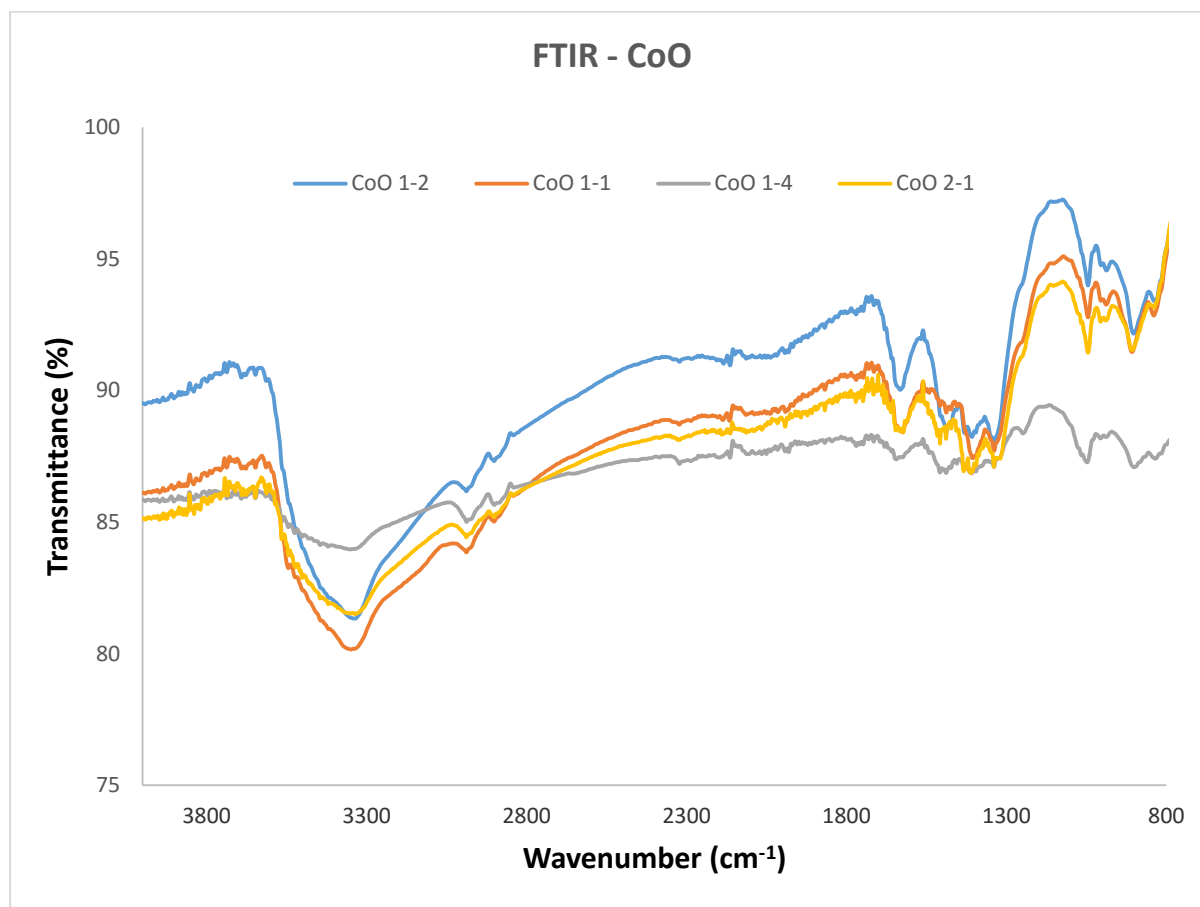


Figure 4.5: FTIR results for Co_3O_4 NPs at different ratios.

FT-IR spectra of synthesised Co_3O_4 with different mole ratios are shown in **Figure 4.5**. All the mole ratio samples shows similar absorption peaks with different intensity. Two distinctive bands at 663 and 576 cm^{-1} are characteristics of the Co-O stretching vibrations in Co_3O_4 . The absorptions at 3424 and 1630 cm^{-1} corresponds to the bending and stretching vibration modes of absorbed water molecules on the surface. It is noted that the bands at approximately 3550 and 1650 cm^{-1} in the FT-IR spectrum of the samples should be assigned to the stretching and bending vibrations of the water molecules absorbed by the samples. Also, there is a tiny band

at approximately 2360 cm^{-1} on the spectrum of some samples due to the presence of atmospheric CO_2 (Farhadi *et al.* 2013).

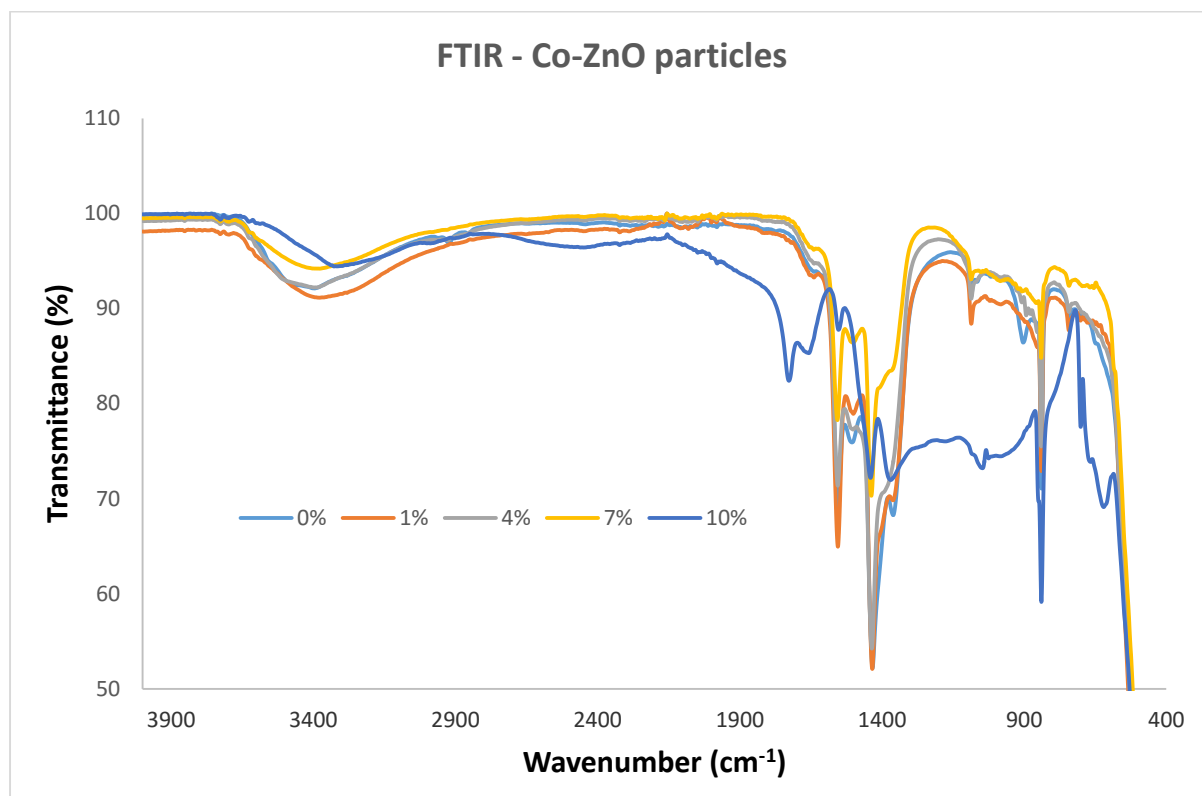


Figure 4.6: FTIR results for Co-ZnO NP from 0- 10%.

Figure 4.6 above shows the FTIR spectrum of Co-ZnO nanoparticles prepared at different doping percentages. The peaks around $2985 - 3000\text{ cm}^{-1}$ correspond to C-H vibration mode of CH_2 groups. The peaks around 1435 cm^{-1} are assigned to OH groups and the surface adsorbed water. This confirms existence of free hydroxyl groups of all the prepared samples, but it has been said doping can improve the surface state of the material and may also generate more surface OH group. In the antimicrobial studies it has been observed previously that the material with the more surface hydroxyl group is the more effective on the inhibition of microorganism. The sharp peak at 1435 cm^{-1} for pure ZnO became more intense and shifted to the upper value when more cobalt was added (Talaat *et al.* 2012).

4.4 Transmission Electron Microscopy

TEM is a very useful technique in characterizing the size and shape of the nanoparticles. Cobalt has been prepared at varied concentrations. The manner in which the reagents attaches itself to Zn and Co metals could have influence on the other surrounding particles, thus affecting the mode of arrangement of the particles.

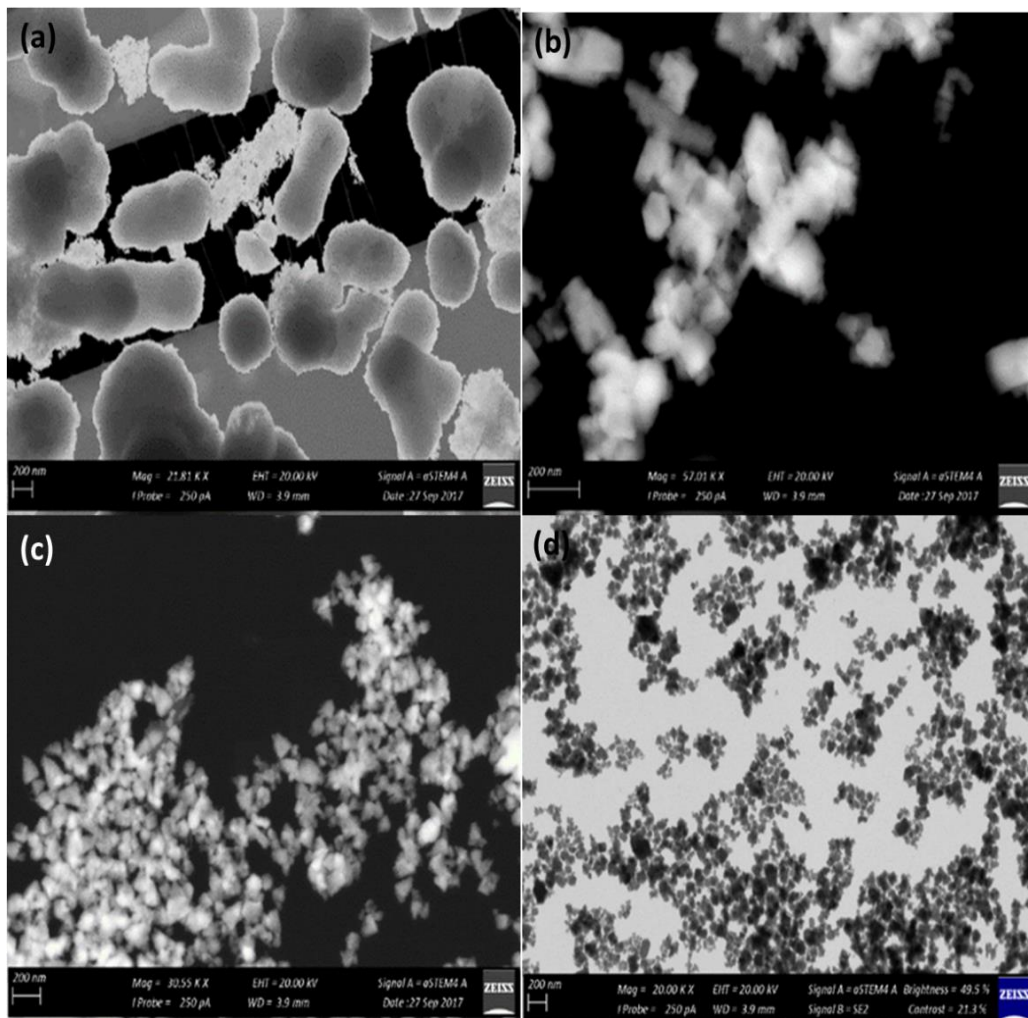


Figure 4.7: TEM results for ZnO NPs at different ratios, (a) 1:1, (b) 1:2, (c) 2:1 and (d) 1:4

The microstructural characterisation studies were conducted to determine the size of the ZnO NPs homogeneity and size distribution (**Figure 4.7**). High resolution transmission electron

micrograph (HRTEM) shows clear platelets with round and hexagonal shapes (for the 1:1 ratio), slightly agglomerated in a chain like network (for ratio 1:2) and mixed shape particles between 50 -100 nm for ratios 2:1 and 1:4 (Marino *et al.* 2012).

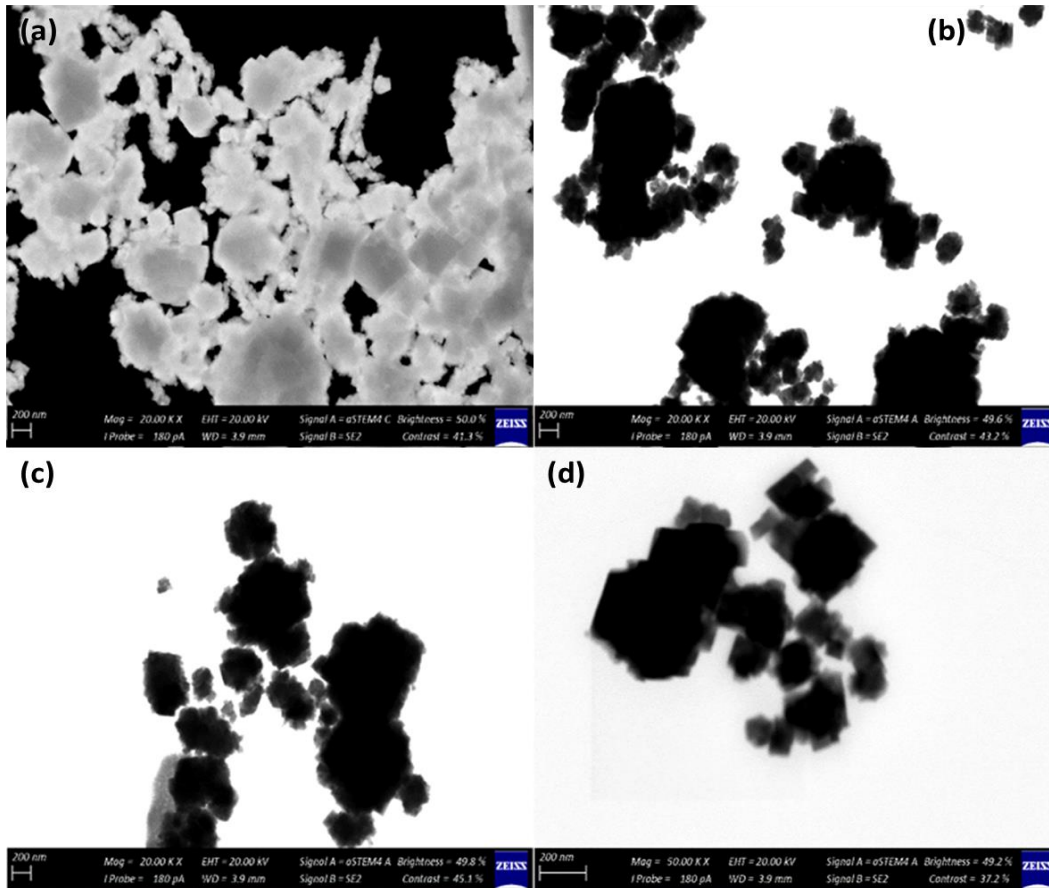


Figure 4.8: TEM results for Co_3O_4 NPs at different ratios (a) 1:1, (b) 1:2, (c) 2:1 and (d) 1:4

HRTEM results for Co_3O_4 (Figure 4.8) shows material that is much agglomerated and is not well dispersed hence the shape cannot be clearly seen (for ratio 1:1). Images had aggregated polycrystalline shape of a particle with narrow size distribution having an irregular shape due to surface particle interaction (ratios 1:2 and 2:1). Some distorted strings were observed for ratio 1:4 due to self-alignment orientation taking place due to the presence of weak interactions. The particles are between 100-200 nm in size (Athar *et al.* 2012).

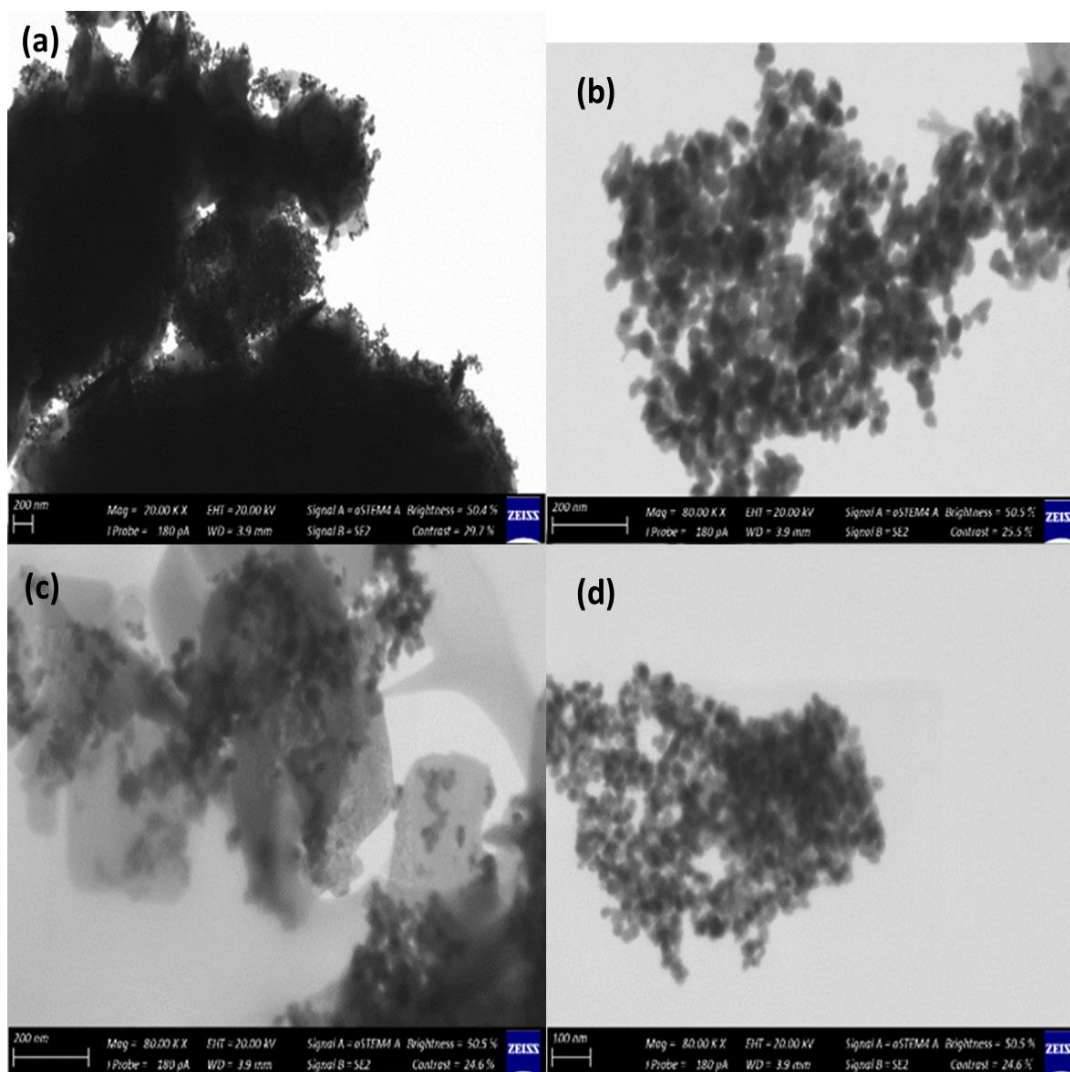


Figure 4.9: TEM results for Co doped ZnO NPs at different percentages (a) 1%, (b) 4%, (c) 7% and (d) 10%

TEM results of Co-ZnO NPs supports the microcrystalline nature of the particle after calcinations with least/ no degree of agglomeration (**Figure 4.9**). Particles are round in shape and they show incorporation of two elements. Other NPs look grey while others are black in color. Grey color is associated with ZnO NPs while black symbolises Co after calcination. It was observed that the annealing temperature increases the crystalline nature of the particle that changes due to nucleation. The particles range from 30 – 50 nm for 4%, 7% and 10% Co doped ZnO (Talaat *et al.* 2012).

4.5 Scanning Electron Microscopy

SEM is a very useful technique in characterizing the morphology of the nanoparticles.

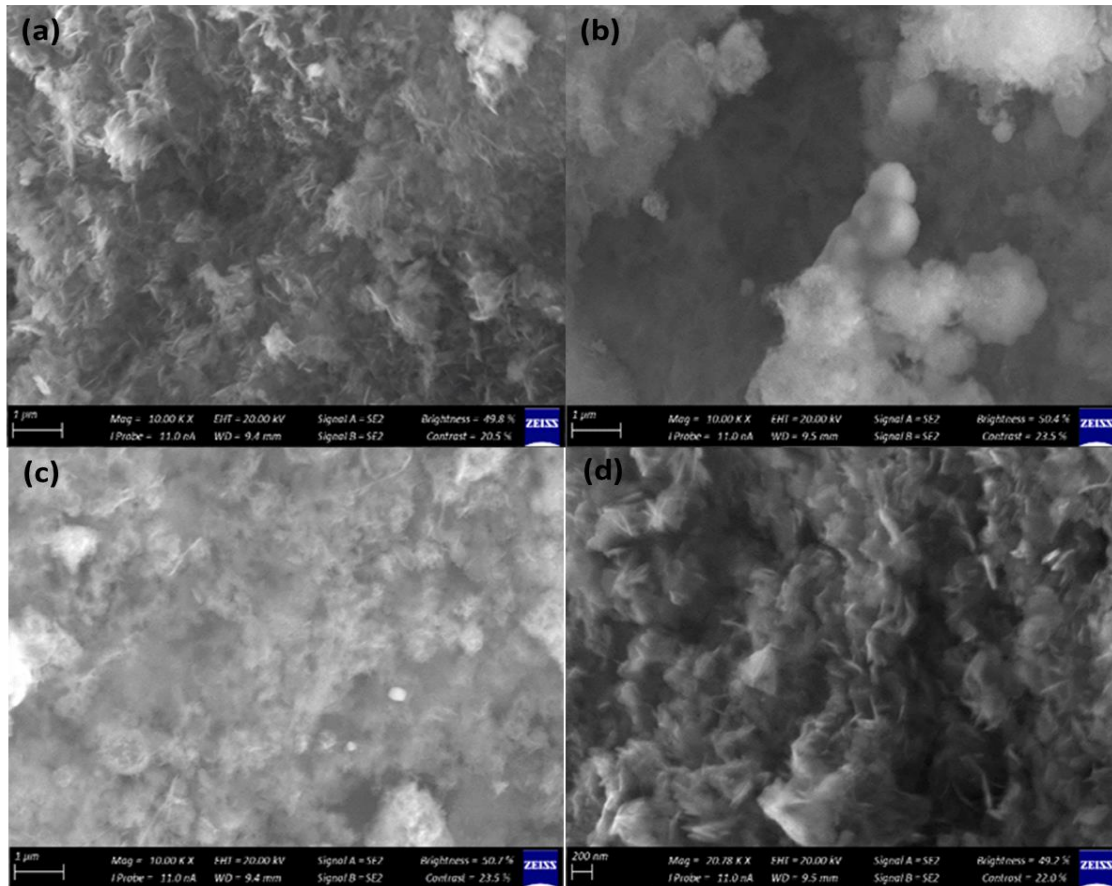


Figure 4.10: SEM results for ZnO NPs at different ratios (a) 1:1, (b) 1:2 (C) 2:1 and (d) 1:4

SEM results of ZnO NPs supports the microcrystalline nature of the particle after calcinations with least degree of agglomeration, as shown in **Figure 4.10**. SEM images revealed mixed shapes for ZnO particles. These images reveal that samples for ratios 1:1 and 1:4 had uniform particles. Agglomerated and mixed shape particles were seen for ratio 1:2 and homogeneous shapes were seen for ratio 2:1 (Marino *et al.* 2012; Kheiralla *et al.* 2014).

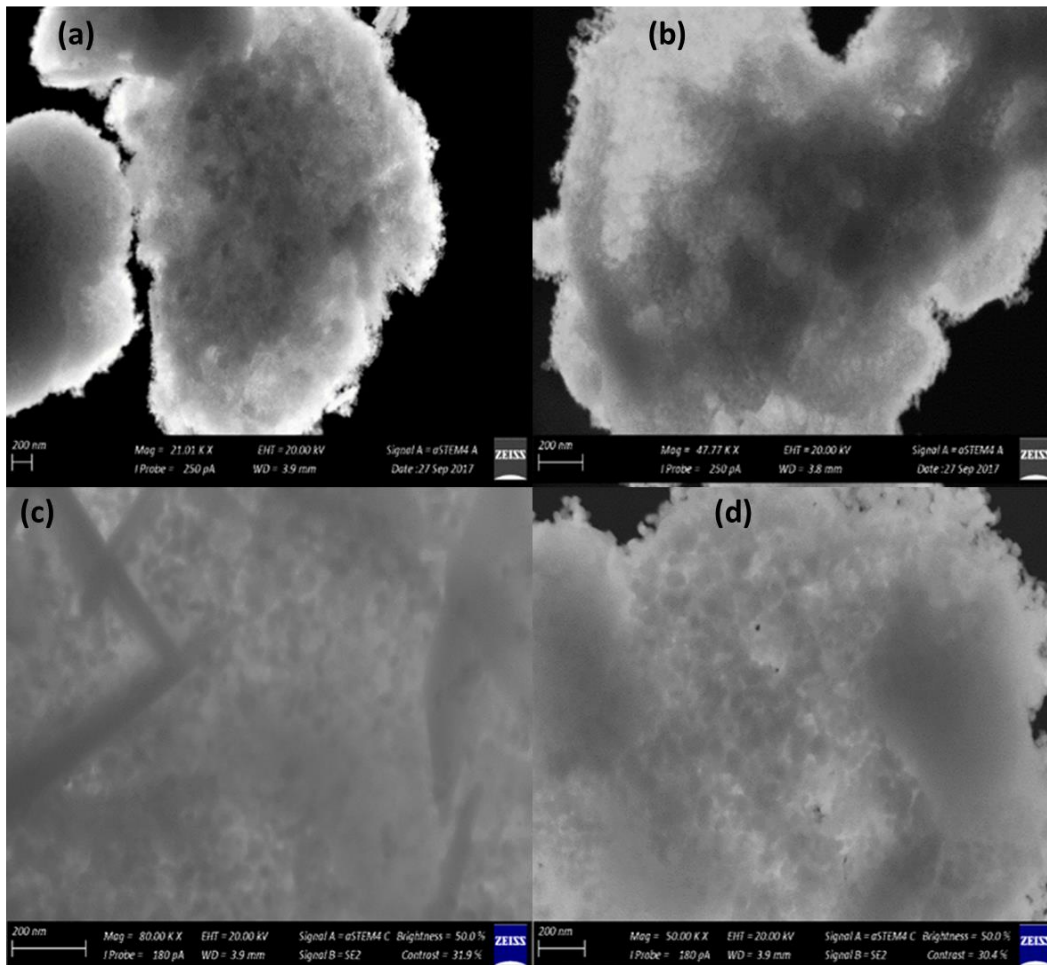


Figure 4.11: SEM results for Co_3O_4 NPs at different ratios (a) 1:1, (b) 1:2 (C) 2:1 and (d) 1:4

SEM results for Co_3O_4 NPs in **Figure 4.11** supports the microcrystalline nature of the particle after calcinations with the least degree of agglomeration. Particles seem to have an irregular shape with chemical homogeneity with uniform morphology due to the presence of inter-particle surface connectivity for all the ratios. It was observed that the annealing temperature increases the crystalline nature of the particle that changes due to nucleation (Yang *et al.* 2003).

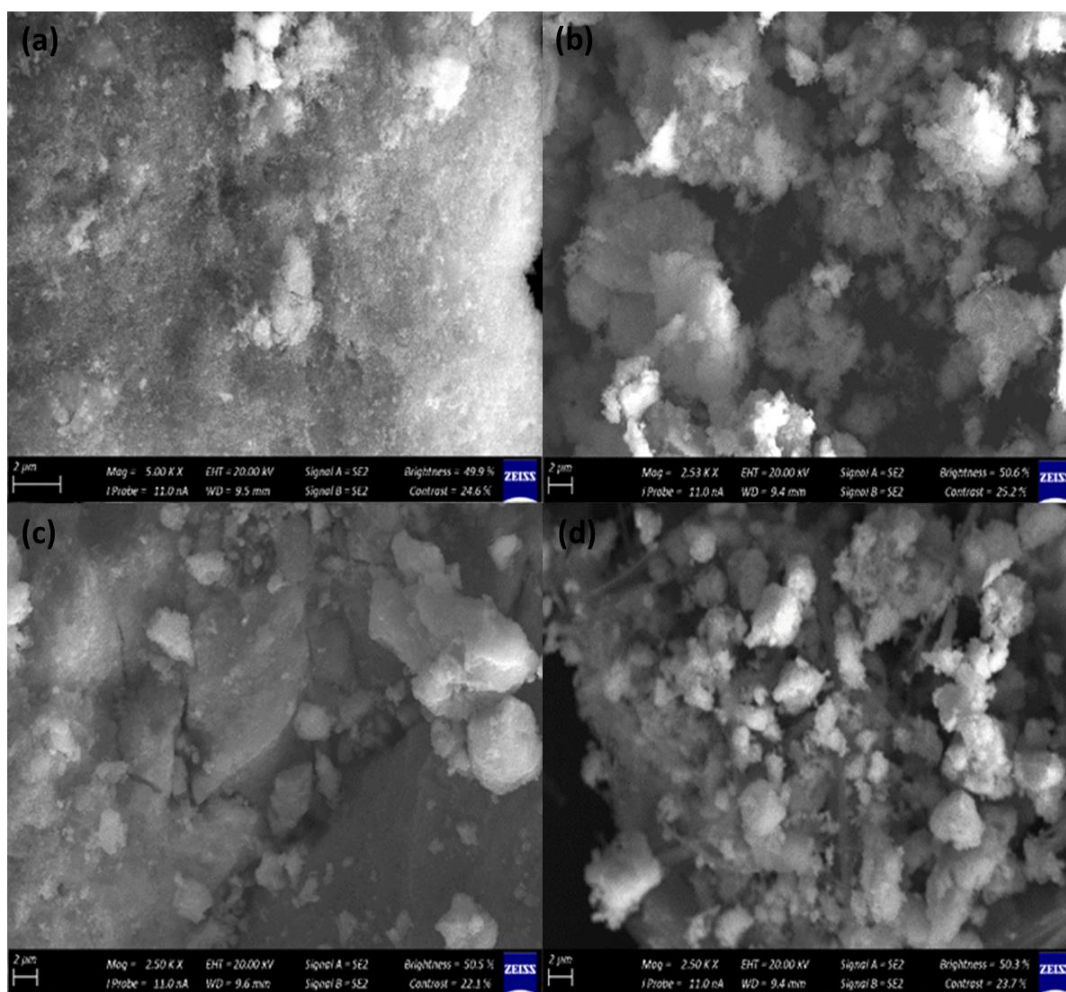


Figure 4.12: SEM results for Co -doped ZnO NPs at different percentages (a) 1%, (b) 4%, (C) 7% and (d) 10%

Particles seem to have an irregular / round shape with chemical homogeneity with uniform morphology due to the presence of interparticle surface connectivity for all the ratios. The annealing of temperature has increased the crystalline nature of the particle that changes due to nucleation, the degree of agglomeration and crystallinity differs in every percentage level of Co as shown in **Figure 4.12** above (Oves *et al.* 2015).

CHAPTER 5

ANTIMICROBIAL RESULTS

5.1 ANTIMICROBIAL TESTS

This chapter deals with the antibacterial activity of the nanomaterials. The antibacterial testing procedures are outlined in Chapter 3. In this chapter data were collected and analysed using the following microorganisms, *S. aureus*, *Shigella sonnei*, *Salmonella enterica* and *Escherichia coli*, pathogenic bacteria and two fungal strains - *Aspergillus niger* and *Candida albicans*.

5.1.1. Disc diffusion assay

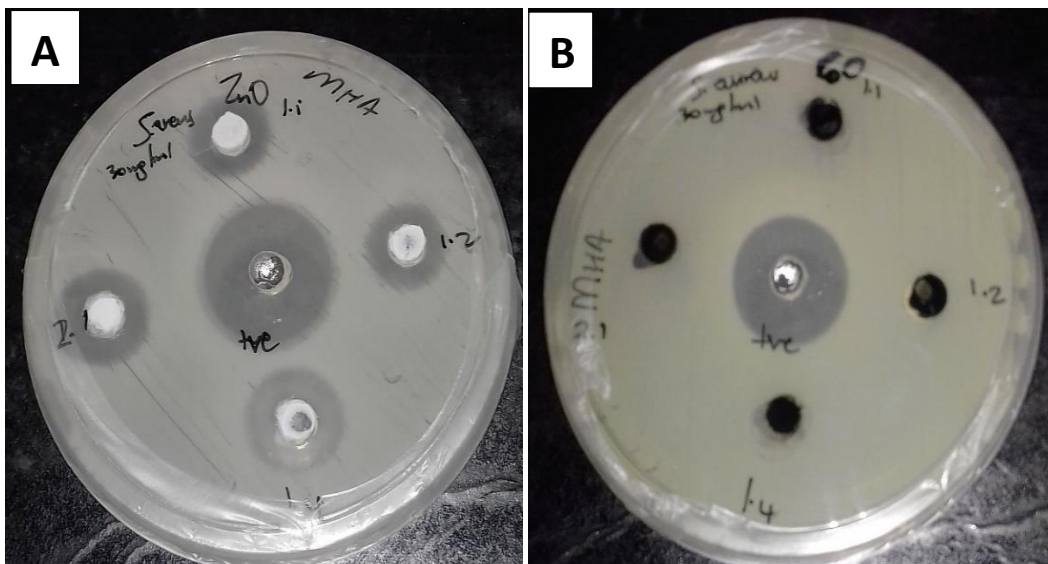
The antibacterial activity of ZnO & Co₃O₄ NPs was tested against Gram-positive bacterium *S. aureus* and Gram-negative bacteria *Shigella sonnei*, *Salmonella enterica* and *E. coli* using different ratios, *ie* 1:1, 1:2, 2:1 & 1: 4 and Co-ZnO NPs at 1%, 4%, 7% and 10% concentration.

MHA diffusion test was performed for antibacterial activity using both Gram-positive bacteria, namely, *Staphylococcus aureus* (*S.aureus*) and Gram-negative bacteria, namely, *Shigella sonnei* (*S. sonnei*), *Salmonella enterica* (*S. enterica*) and *Escherichia coli* (*E. coli*). The antibacterial activity was expressed in terms of the diameter of the zone of inhibition. The zones were used for the determination of effectiveness of the synthesised nanoparticles (Shivananda *et. al.* 2016).

5.1.2. Antibacterial activity of selected bacterial strains

The results below (Figures: 5.1- 6.) indicate that the working concentration of NPs, which is 2 mg/ml was not effective against any of the bacterial species used in the test. However, the colloidal solutions of the positive control (Neomycin) antibiotic exhibited the growth inhibitory effect against both Gram-positive and Gram-negative bacterial species used in the study. Though positive control induced bacterial growth inhibition, all bacterial species were not equally sensitive.

The advantage of the well diffusion assay is that you can usually load more sample at one time into a well, compared to loading a disc. The results of the quantitative antimicrobial assessment by well diffusion method are reported in **Table 5.1** and **Figures (5.1)** from which it is observed that the size of the inhibition zone by Neomycin is larger than the one formed by NPs isolated at 30 mg/ml. The reason for the difference in the antibacterial activity for different test microorganisms may be due to the difference in structure and thickness of the cell wall (Navale *et al.* 2015).



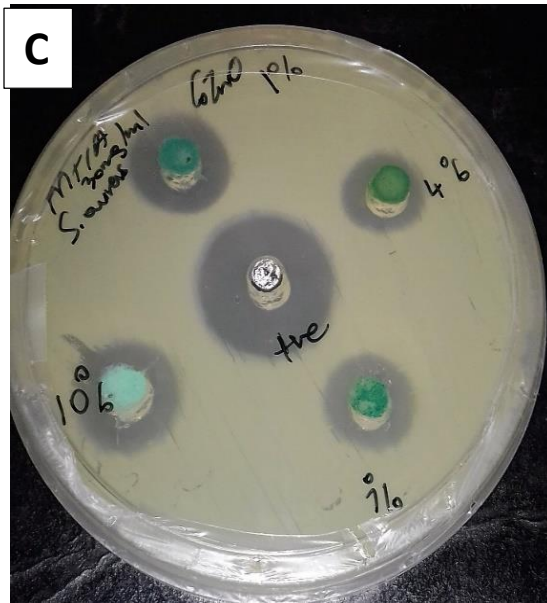


Figure 5.1: Antibacterial activity (zone of inhibitions) of the biosynthesised (A) ZnO, (B) Co₃O₄ (C) Co-ZnO NPs against *S. aureus*

After incubating plates inoculated with *S. aureus* for 24 hrs against different concentrations of the NPs, there were zones of inhibition for ZnO and Co-ZnO NPs **Figure (5.1. A and C)**. Zones of inhibition are summarised in **Table 5.1**. It shows that these NPs have antibacterial activity. ZnO NPs shows different zones of inhibition at different ratios. Ratio 1:4 has the biggest zone than the rest of ZnO ratios, so it can be considered as the most effective ratio. It showed considerable antibacterial activity with the inhibition zones ranging from 3 mm- 5 mm diameter. In the case of (C) Co-ZnO NPs against *S. aureus*, results shows that 7% is more effective for inhibition of bacteria than the other percentages used. It also showed antibacterial with the inhibition zones ranging from 3 mm - 5 mm in diameter. However, these NPs have zones of inhibition which are less than the one for broad spectrum antibiotic (Neomycin) which is used as positive (+ve) control. The diameter of inhibition ranges from 9 mm - 10 mm (Savithamma *et al.* 2016).

ZnO and Co-ZnO NPs have the ability to bind to proteins and DNA and damage them by inhibiting replication of *S. aureus*. They attack the respiratory chain, cell division finally leading to cell death. These nanoparticles release Zn ions and oxygen reactive species (ORS) in the bacterial cells, which enhance their bactericidal activity (Feng *et al.* 2000; Sondi and Salopek- Sondi 2004; Song *et al.* 2006).

In addition, complex action mechanisms of metals decrease the probability of bacteria developing resistance to them (Chopra 2007). Thus, one of the promising approaches for overcoming antibiotic resistance of microorganisms is the use of ZnO nanoparticles. The association of metal oxide nanoparticles and antibiotics is a very promising area of research. ZnO nanoparticles are interesting in the field of Medicine (Li *et al.* 2005). Co₃O₄ NPs did not inhibit a single organism, therefore, it is not effective for microbial inhibition.

Table 5.1: Mean zones of inhibition (in mm) produced by synthesised ZnO, Co₃O₄ and Co-ZnO NPs against *S. aureus*

Bacteria used for biosynthesis of nanoparticles	Nanoparticle used	Zone of inhibition (mm) caused by NPs				Neomycin antibiotic (2mg/ml)
		1:1	1:2	1:4	2:1	
<i>S. aureus</i>	ZnO (30 mg/ml) at different ratios	1:1	1:2	1:4	2:1	
		4	3	5	4	10
	Co ₃ O ₄ (30 mg/ml) at different ratios	1:1	1:2	1:4	2:1	
		-	-	-	-	9
	Co-ZnO (30 mg/ml) at different percentages	1%	4%	7%	10%	
		3	4	5	4	9

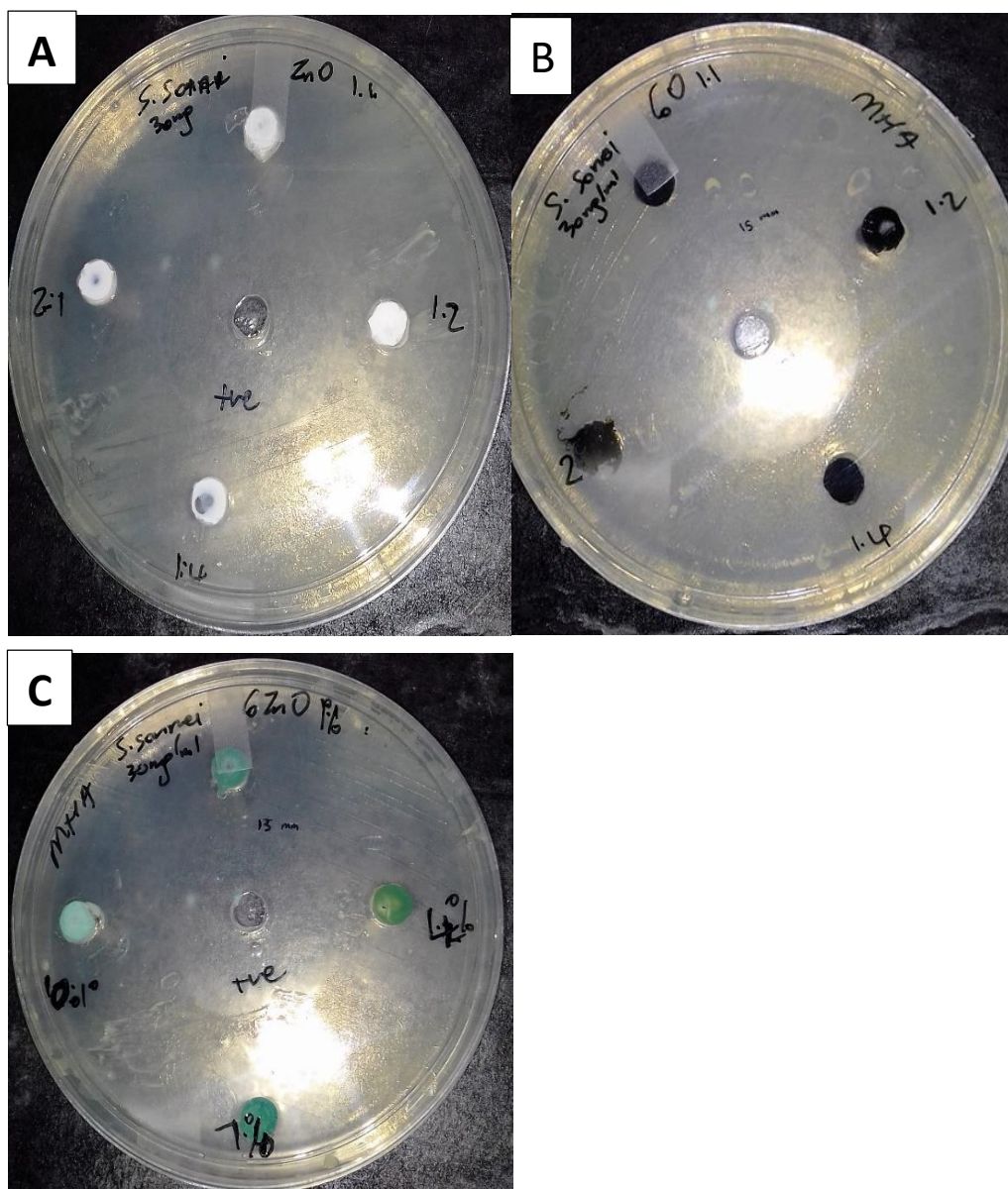


Figure 5.2: Antibacterial activity of the biosynthesised (A) Co_3O_4 , (B) ZnO and (C) Co-ZnO NPs nanoparticles against *S. sonnei*

S. sonnei was incubated for 48 h because it grows very slow than the rest of the bacterial strains used on the study. After incubating plates inoculated with *S. sonnei* for 48 h against different concentrations of the NPs, there were no zones of inhibition for all NPS as shown in **Figure (5.2 .A - C)**. Zones of inhibition are summarised in Table 5.2. It shows that these NPs had no antibacterial activity against *S. sonnei*. The reason for the difference in the antibacterial activity for different test microorganisms

may be due to the difference in structure and thickness of the cell wall. Neomycin, which is used as positive (+ ve) control shows diameter of inhibition rages from 13 mm- 15 mm (Navale *et al.* 2015).

Table 5.2: Mean zones of inhibition (in mm) produced by synthesised ZnO, Co₃O₄ and Co-ZnO NPs against *S. sonnei*

Bacteria used for biosynthesis of nanoparticles	Nanoparticle used	Zone of inhibition (mm) caused by NPs				Neomycin antibiotic (2mg/ml)
		1:1	1:2	1:4	2:1	
<i>S. sonnei</i>	ZnO (30 mg/ml) at different ratios	1:1	1:2	1:4	2:1	
		-	-	-	-	13
	Co ₃ O ₄ (30 mg/ml) at different ratios	1:1	1:2	1:4	2:1	
		-	-	-	-	15
	Co-ZnO (30 mg/ml) at different percentages	1%	4%	7%	10%	
		-	-	-	-	13

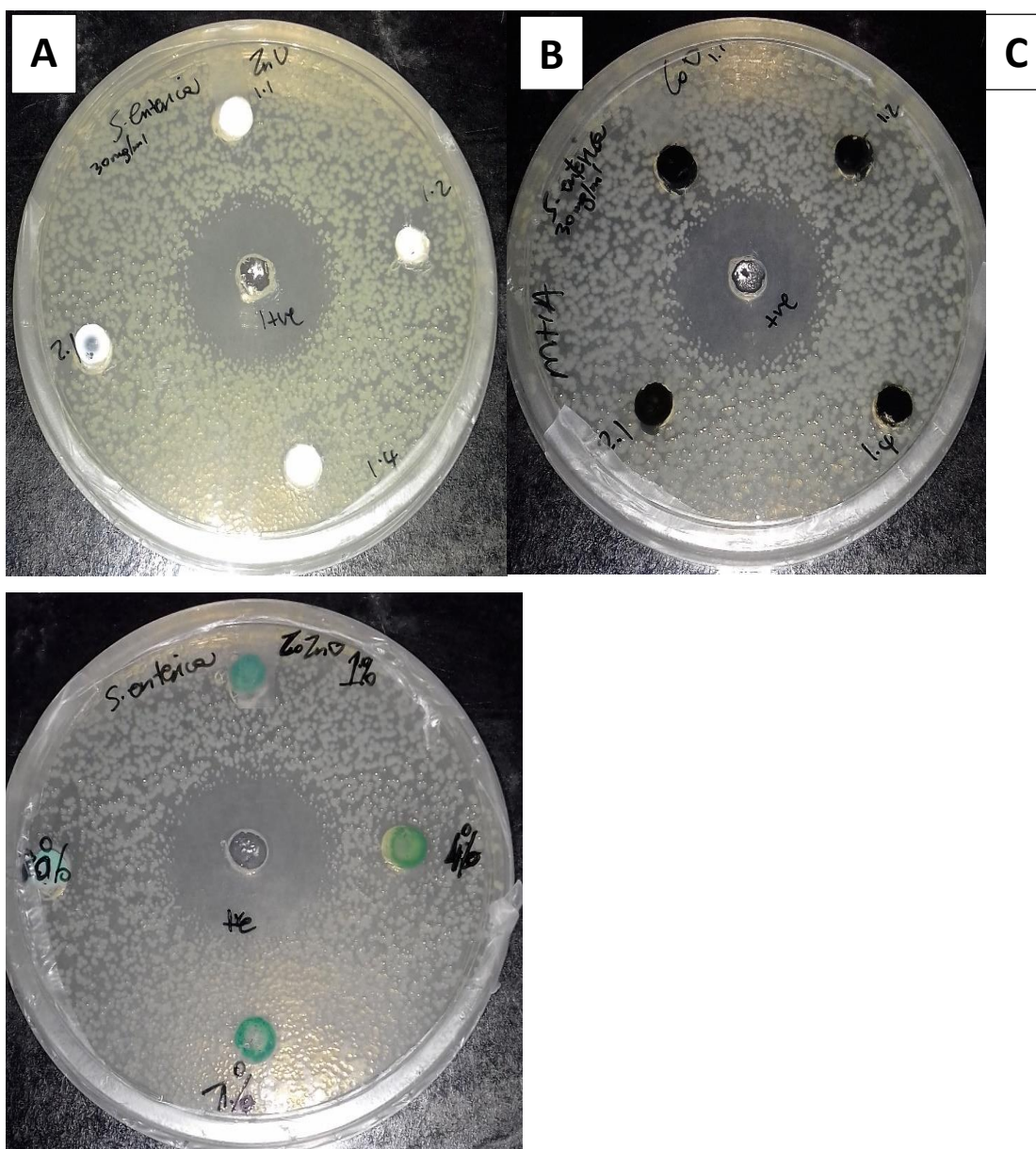


Figure 5.3: Antibacterial activity of the biosynthesised (A) ZnO (B) Co_3O_4 , and (C) Co-ZnO NPs against *S. enterica*

After incubating plates inoculated with *S. enterica* for 24 hrs against different concentrations of the NPs, there were no zones of inhibition for all NPS as shown in **Figure (5.3 A - C)**. Zones of inhibition are summarised for positive control in **Table 5.3**. It shows that these NPs had no antibacterial activity against *S. enterica*. The reason for the difference in the antibacterial activity for different test microorganisms may be

due to the difference in structure and thickness of the cell wall. Neomycin shows diameter of inhibition ranges from 10 mm- 11 mm (Navale *et al.* 2015).

Table 5.3: Mean zones of inhibition (in mm) produced by synthesised ZnO, Co₃O₄ and Co-ZnO NPs against *S. enterica*

Bacteria used for biosynthesis of nanoparticles	Nanoparticle used	Zones of inhibition (mm) caused by NPs				Neomycin antibiotic (2mg/ml)
		1:1	1:2	1:4	2:1	
<i>S. enterica</i>	ZnO (30 mg/ml) at different ratios	1:1	1:2	1:4	2:1	
		-	-	-	-	10
	Co ₃ O ₄ (30 mg/ml) at different ratios	1:1	1:2	1:4	2:1	
		-	-	-	-	11
	Co-ZnO (30 mg/ml) at different percentages	1%	4%	7%	10%	
		-	-	-	-	11

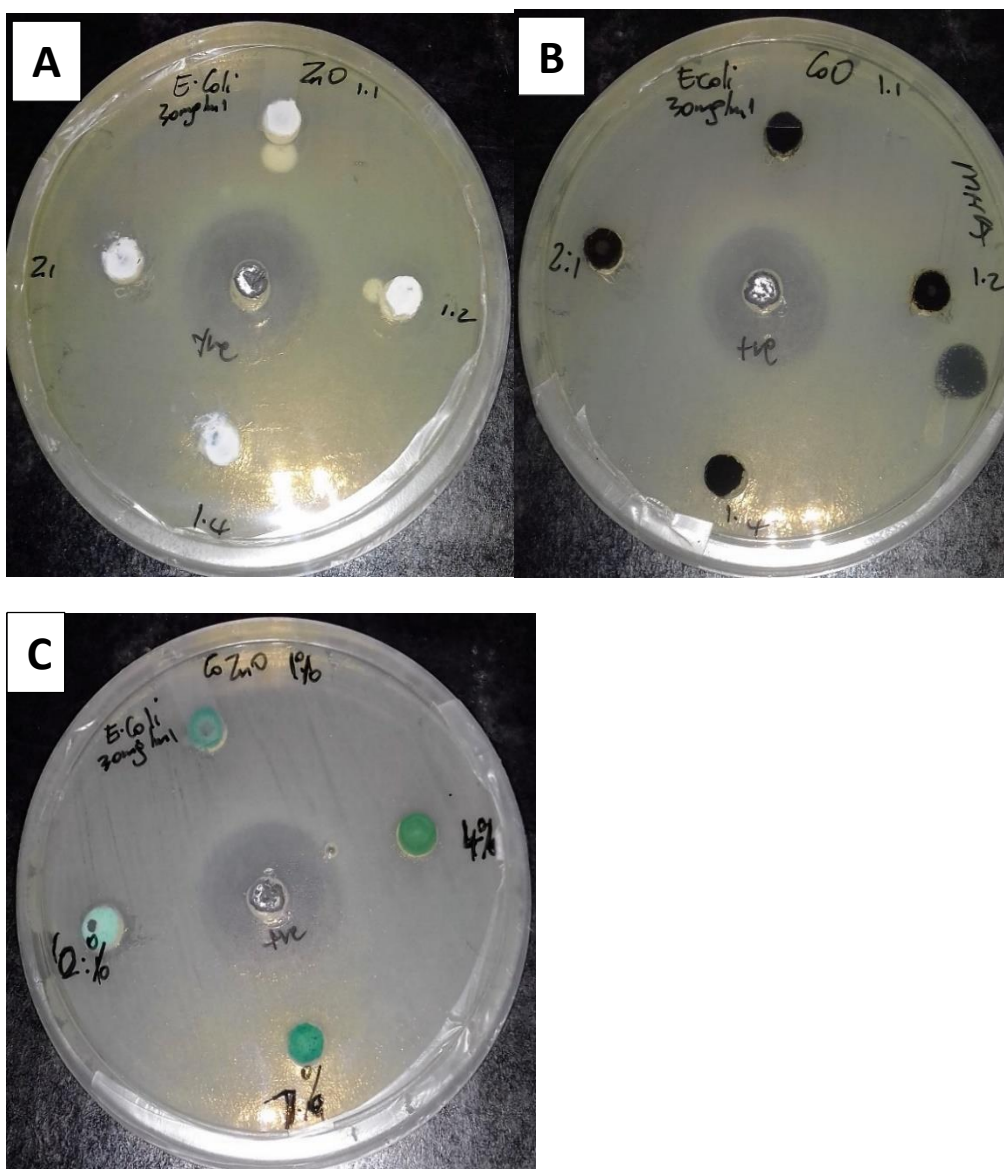


Figure 5.4: Antibacterial activity of the biosynthesised (A) ZnO (B) Co₃O₄, and (C) Co-ZnO NPs against *E. coli*

After incubating plates inoculated with *E. coli* for 24 hrs against different concentrations of the NPs, there were no zones of inhibition for (A) ZnO and (B) Co₃O₄ NPs as shown in **Figure (5.4 A and B)**. Co-ZnO showed a little zone of inhibition which is 1 mm only at 10% concentration. It shows that these NPs have little antibacterial activity against *E. coli* at 30 mg/ml. Zones of inhibition are summarised for positive control in Table 5.4. ZnO and Co₃O₄ NPs did not show any antibacterial

activity against *E. coli*. Neomycin shows a zone of inhibition that ranges from 10 mm- 11 mm. Though positive control induced bacterial growth inhibition, all bacterial species were not equally sensitive as shown in **Table 5.4**.

Table 5.4: Mean zone of inhibition (in mm) produced by synthesised ZnO, Co₃O₄ and Co-ZnO NPs against *E. coli*

Bacteria used for biosynthesis of nanoparticles	Nanoparticle used	Zones of inhibition (mm) caused by NPs				Neomycin antibiotic (2mg/ml)
		1:1	1:2	1:4	2:1	
<i>E. coli</i>	ZnO (30 mg/ml) at different ratios	1:1	1:2	1:4	2:1	
		-	-	-	-	10
	Co ₃ O ₄ (30 mg/ml) at different ratios	1:1	1:2	1:4	2:1	
		-	-	-	-	11
	Co-ZnO (30 mg/ml) at different percentages	1%	4%	7%	10%	
		-	-	-	1	11

5.2. Antifungal activity of the NPs

The increase in fungal infections has prompted an increase in the use of antifungal agents, and in practice the widespread clinical use of these agents has resulted in measurable rates of acquired or innate fungal resistance in *Candida* species (Eksi, Gayyurhan and Balci 2013). Even though Amphotericin B is one of the most toxic antimicrobial agents in clinical use, it still qualifies as a standard treatment. Resistance was reported in nonalbicans *Candida* species, for example, species *C. lusitaniae* and *C. guilliermondii* (Swinne *et al.* 2004). Clinical failure to respond to Amphotericin B treatment occurs with recovery of the factors about the immune system of the host rather than with in vitro resistance (Arikan and Rex 2007). Amphotericin B resistance

may vary by region, and the resistance profile may also vary at different times in the same region.

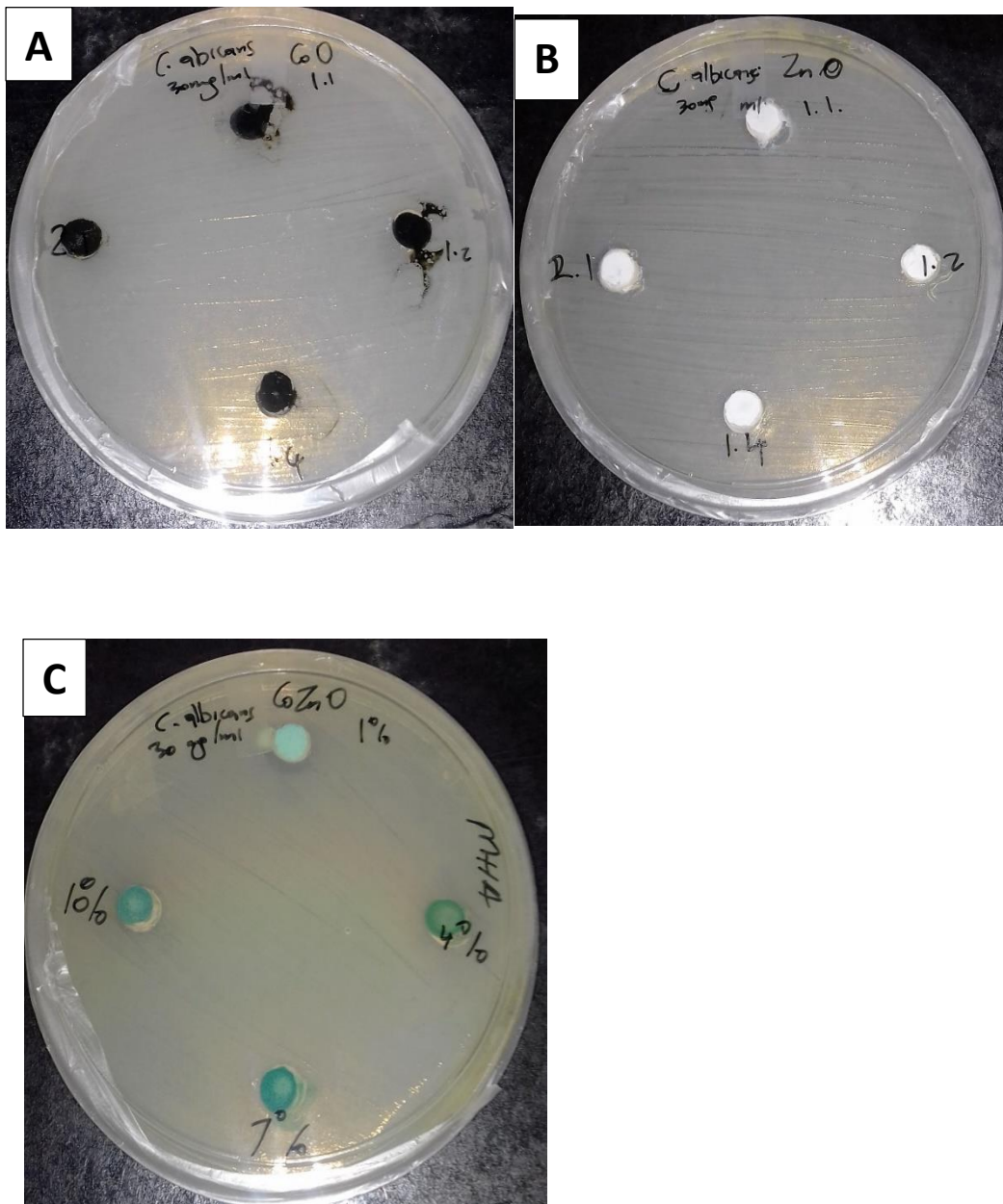


Figure 5.5: Antifungal activity of the biosynthesised (A) ZnO (B) Co_3O_4 , and (C) Co-ZnO NPs against *C. albicans*

After incubating plates inoculated with *C. albicans* for 48 h at 25°C together with different concentrations of the NPs, there were no zones of inhibition for all the NPs

as shown in **Figure (5.5 A -C)**. It shows that these NPs have little/ no antifungal activity against *C. albicans* at 30 mg/ml.

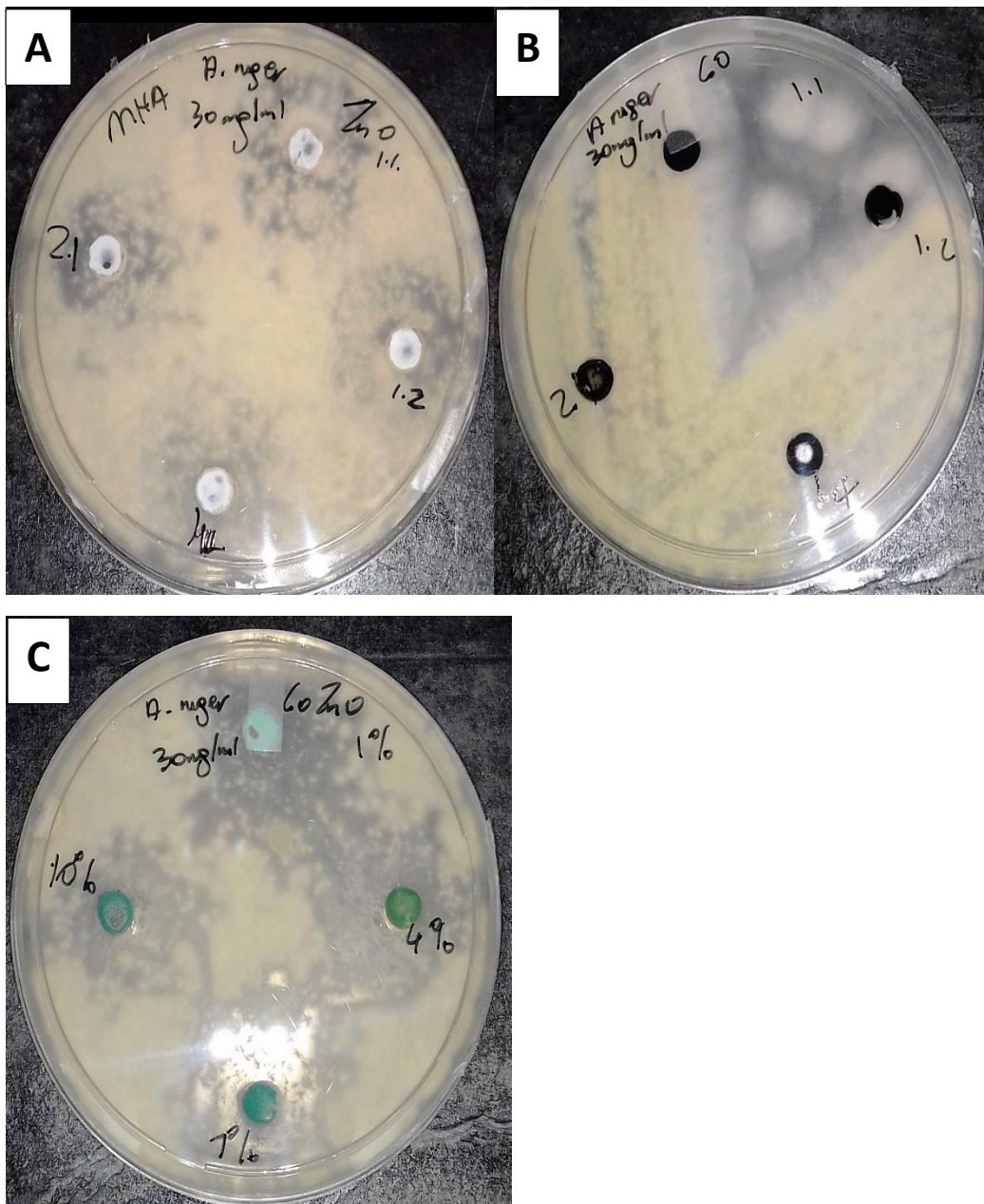


Figure 5.6: Antifungal activity of the biosynthesised (A) ZnO (B) Co₃O₄, and (C) Co-ZnO NPs against *A. niger*

The results in **Figure 5.6** indicated that ZnO and Co-ZnO have partially inhibited the growth of *A. niger* at a concentration of 30 mg/ml. The antifungal activity was found to depend strongly on the concentration. According to Diasty *et al.* (2013), the presence of high inhibition zone

with nearly no growth occurrence against tested strains clearly indicate that the mechanism of the fungicidal action of ZnO involves disrupting the membrane. The results are also detailed in **Table 5.5**, where Co₃O₄ did not show any antimicrobial activity. These results agree with those obtained by Lipovsky *et al.* (2011), who recorded the ability of ZnO nanoparticles to affect the viability of the pathogenic yeast, *Candida albicans*, as well as a concentration-dependent effect.

Table 5.5: Mean zones of inhibition (in mm) produced by synthesised ZnO, Co₃O₄ and Co-ZnO NPs against *A. niger*

Bacteria used for biosynthesis of nanoparticles	Nanoparticle used	Zones of inhibition (mm) caused by NPs			
		1:1	1:2	1:4	2:1
<i>A. niger</i>	ZnO at different ratios	1:1	1:2	1:4	2:1
		Slightly growth	Slightly growth	Slightly growth	Slightly growth
	CoO at different ratios	1:1	1:2	1:4	2:1
		-	-	-	-
	Co-ZnO different Ratios	1%	4%	7%	10%
		Slightly growth	Slightly growth	Slightly growth	Slightly growth

According to Savithramma *et al.* (2011), the minimal fungicidal concentration of ZnO was found to be 0.1 mg/mL. This concentration caused an inhibition of over 95% in the growth of *C. albicans*. ZnO nanoparticles also inhibited the growth of *C. albicans* when it was added at the logarithmic phase of growth. Sawai and Yoshikawa in 2004, evaluated antifungal activity of metallic oxides (MgO, CaO and ZnO) by an indirect conductimetric assay. Their results indicated that CaO and MgO had antifungal activity above 1600 ppm against *S. cerevisiae* and other fungi. However, ZnO exhibited only a weak antifungal activity against *S. cerevisiae*, but some growth inhibition was observed at 100 ppm.

Shi *et al.* (2010), mentioned that ZnO nanoparticles had fungicidal effect against yeasts and also a fungistatic action against moulds. The difference between yeasts and moulds could be attributable to the difference in their cell wall and membrane structure. Chitin makes up to 45% of the cell wall of *Aspergillus niger*. However, it is present only 3% in *Saccharomyces cerevisiae*. For almost all fungi, the central core of the cell wall is a branched β -1, 3, 1, 6 glucan that is linked to chitin via a β -1, 4 linkage. The binding of the oxides particles on the fungal cell surface through electrostatic interactions could be a possible mechanism.

Disc or well diffusion tests are both qualitative assays. Hence, they will not give an accurate estimation of the effect of the antimicrobial activity. Minimal Inhibitory Concentration (MIC) values must be investigated for quantitative estimation.

5.2. Minimum inhibitory concentration

In microbiology, the minimum inhibitory concentration (MIC) is the lowest concentration of a chemical, usually a drug, which prevents visible growth of bacterium. MIC depends on the microorganism, the affected human being (*in vivo* only), and the antibiotic itself.

The antibacterial activity of ZnO, Co₃O₄ and Co- doped ZnO NPs was tested against *S. aureus*, *Shigella sonnei*, *Salmonella enterica* and *E. coli* using different ratios, *ie* 1:1, 1:2, 2:1 & 1: 4. The minimum concentration of the ZnO, Co₃O₄ and Co- doped ZnO NPs colloidal samples, which can effectively inhibit the growth of tested pathogens, is known as MIC values of that particular sample. When the sample has low MIC value it is known to have good antibacterial activity. The sample concentration, which inhibits the growth of tested pathogen, can be identified by color change (pink to blue) when using resazurin dye. That blue color indicates bacterial growth inhibition and is also known as MIC value as shown from Figure 5.7. It is followed by wells below whereby the pink color indicates the growth of

microorganisms. The ZnO NPs are more effective at inhibiting pathogenic organisms and all MIC results are listed in Table 5.6. The synthesised Co_3O_4 NPs did not inhibit growth of *S. aureus* and *S. sonnei*.

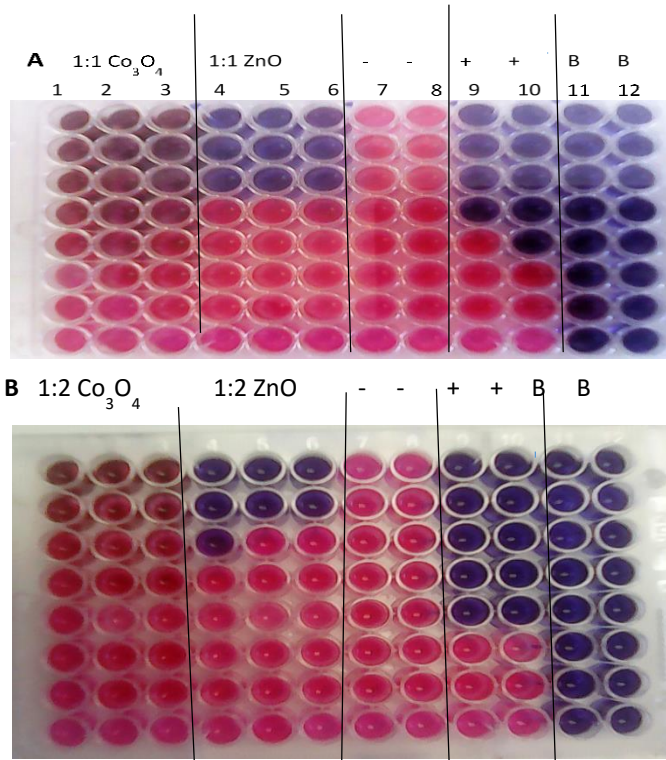


Figure 5.7: MIC results for *S. sonnei* against Co_3O_4 and ZnO NPs at ratio 1:1 and 1:2 MIC plates after 18- 24 h of incubation in modified resazurin assay. Pink colour indicates growth of microorganism, blue symbolises inhibition of growth. Column 1-6 (C 1- 6) NPs, C (7-8) negative control, C (9-10) positive control (Neomycin 2 mg/ml) and C (11- 12) broth sterility test.

In Figure 5.7, MIC results show that only ZnO NPs effective against *S. sonnei* C (4- 6) and MIC at ratio 1:1 is 6.25 $\mu\text{g}/\text{ml}$ and 12.5 $\mu\text{g}/\text{ml}$ for ratio 1: 2. This claim is supported by the appearance of the purple colour. However, neomycin as a positive control was effective against all the organisms as compared to the nanoparticles used. This indicates that the *S. sonnei* is more susceptible to positive control than all the nanoparticles tested (Bryner *et al.* 2006). The Co_3O_4 NPs did not inhibit the growth of *S. sonnei* C (1- 3) at both ratios. It can be concluded

that synthesised Co_3O_4 NPs has less or no antibacterial activity as shown on the MIC plate above. After this plate, more attention and focus was on ZnO NPs hence they exhibited the antimicrobial activity on MIC plate.

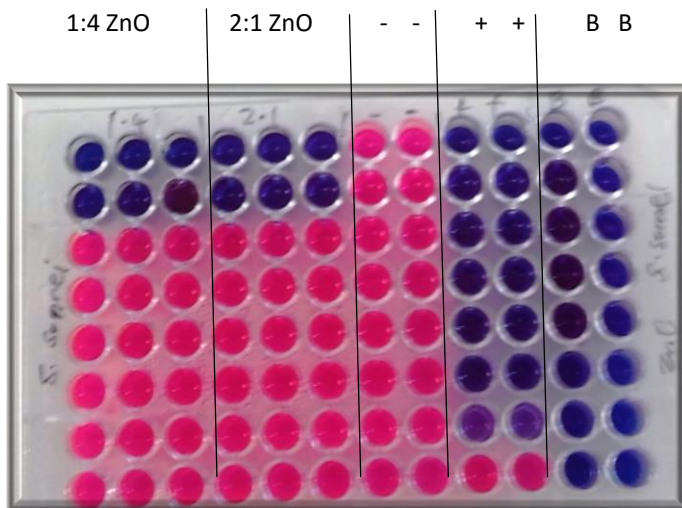


Figure 5.8 MIC results for *S. sonnei* against ZnO NPs at ratio 1:4 and 2:1.

Figure 5.8 shows the MIC of ZnO NPs at ratio 1:4 (C1- C3) & 2:1(C4- C6) on *S. sonnei*. The results show these nanoparticles were effective against *S. sonnei* at ratios tested. This claim is supported by the appearance of the purple colour on the MIC plates. However, neomycin as a positive control was more effective against all the organisms as compared to ZnO nanoparticles. This indicates that the *S. sonnei* is more susceptible to positive control than all the nanoparticles tested (Bryner *et al.* 2006). More attention has been given to ZnO hence it possesses inhibitory effect, for ratio 1:4 and 2:1.

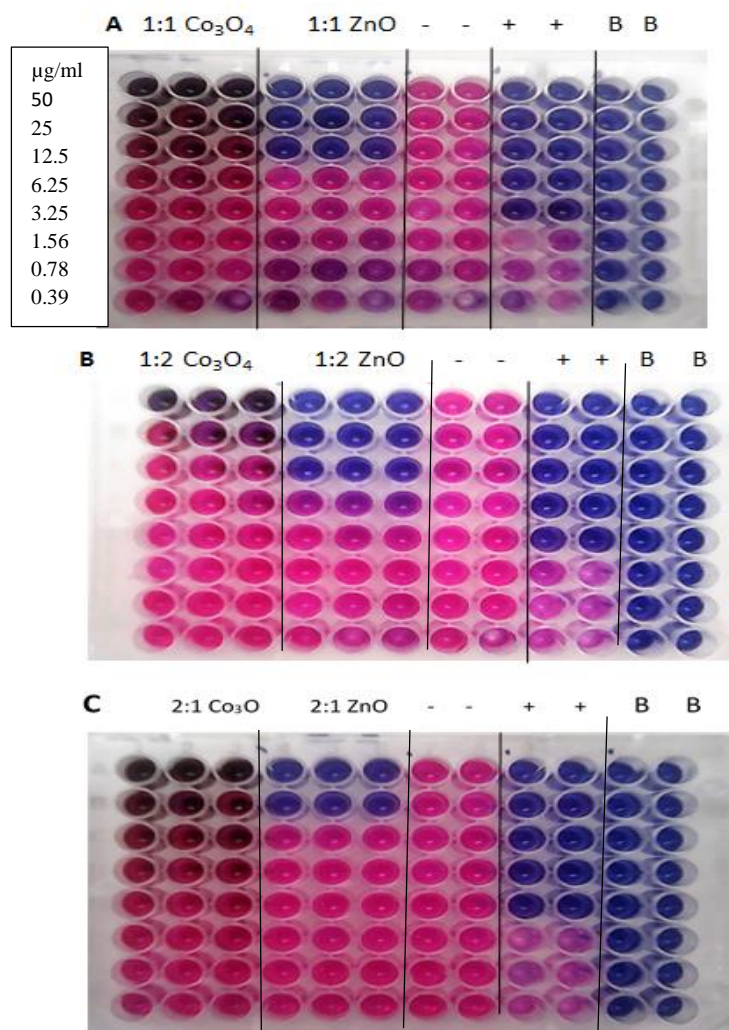


Figure 5.9: MIC results for *S. aureus* against Co_3O_4 and ZnO NPs at ratio 1:1, 1:2 and 2: 1

In Figure 5.9 MIC results show that only ZnO NPs were effective against *S. aureus* with the MIC of 6.25 $\mu\text{g/ml}$ at ratio 1:1 and 1:2 and 12.5 $\mu\text{g/ml}$ at ratio 2:1. The Co_3O_4 NPs did not inhibit the growth of *S. aureus* at ratio 1:1, 1:2 and 2:1. This claim is supported by the appearance of the purple colour. On the other side, neomycin as a positive control was effective against all the organisms as compared to nanoparticles used. It can be concluded that synthesised Co_3O_4 NPs have little or no antibacterial activity as shown on the MIC plate (Zang *et al.* 2008).

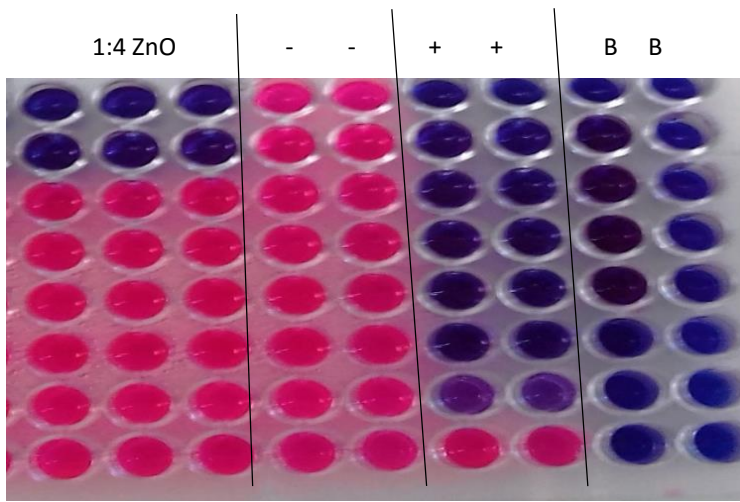


Figure 5.10: MIC results for *S. aureus* against ZnO NPs at ratio 1: 4.

In Figure 5.10, *S. aureus* cells were rendered non-viable after treatment with 25 $\mu\text{g/ml}$ nanoparticles. This indicates that *S. aureus* is more susceptible to the antimicrobial effects of neomycin than ZnO, results agree to the paper reported by Zang *et al.* (2008). This indicates that the *S. aureus* is more susceptible to positive control than all the nanoparticles tested

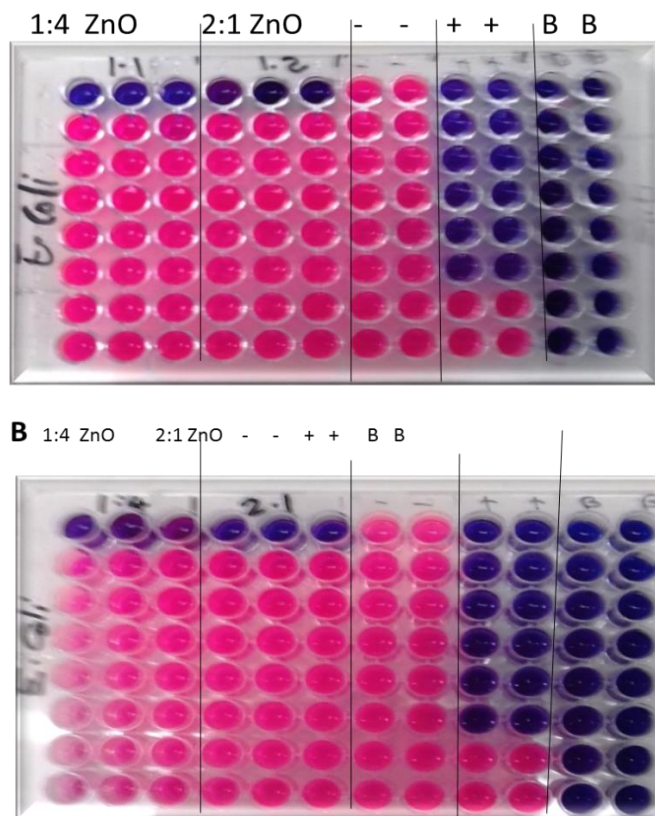


Figure 5.11. MIC results for *E. coli* against ZnO NPs at ratio 1:1, 1:2, 1:4 and 2:1

Figure 5.11 have shown that ZnO NPs are effective against *E. coli* and MIC is 25 $\mu\text{g}/\text{ml}$ for all the ratios tested. This claim is supported by the appearance of the purple colour. However, neomycin as a positive control was effective against all the organisms as compared to all the three nanoparticles. According to the studies made by Zang *et al.* (2008), these results indicate that the *E. coli* is more susceptible to positive control than all the nanoparticles tested.

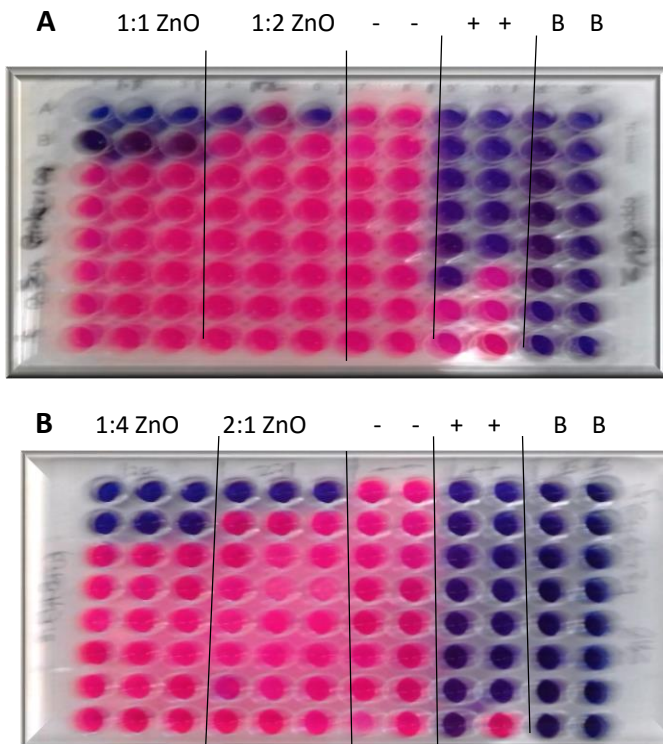


Figure 5.12. MIC results for *S. enterica* against ZnO NPs at ratio 1:1, 1:2, 1:4 and 2:1.

Figure 5.12 have shown that ZnO NPs are effective against *S. enterica* and MIC for ratio 1:1 and 1:4 is 12.5 $\mu\text{g}/\text{ml}$ and for ratio 1:2 and 2:1 is 25 $\mu\text{g}/\text{ml}$ respectively. This claim is supported by the appearance of the purple colour. However, neomycin as a positive control was effective against all the organisms as compared to all the three nanoparticles. This indicates that the *S. enterica* is more susceptible to positive control than all the nanoparticles tested. These results agree with the report given by Vijayaraghavan in 2010. All the bacterial MIC concentrations are recorded in Table 5.6 below.

TABLE 5.6: MIC values of synthesised ZnO and Co₃O₄ NPs at different ratios against selected bacterial strains.

		MIC values (µg/ml)			
		Bacterial strains			
Sample name	Ratio	<i>Staphylococcus aureus</i>	<i>Shigella. Sonnei</i>	<i>Escherichia coli</i>	<i>Salmonella enterica</i>
ZnO	1:1	6.25	6.25	25	12.5
ZnO	1:2	6.25	12.5	25	25
ZnO	1:4	12.5	12.5	25	12.5
ZnO	2:1	12.5	12.5	25	25
Co ₃ O ₄ (same ratios)	All	No MIC	No MIC	No MIC	No MIC
Co-doped-ZnO 1, 4, 7 & 10 %	All	No MIC	No MIC	No MIC	No MIC

Table 5.6 shows that ZnO NPs had significantly enhanced antibacterial activity in all the ratios, (1:1 MIC is 6.25, 1:2 MIC is 6.25, 1:4 MIC 12.5 and 2:1 12.5 µg/ ml) against *Staphylococcus aureus*, as shown in Figure 5.9 . It also inhibited *Shigella sonnei* with MIC values ranging from 6.25- 12.5 µg/ml (Fig. 5.7- 8), *Salmonella enterica* with MIC values ranging from 12.5- 25 µg/ml (Fig. 5.10) and *Escherichia coli* with the MIC values of 25 µg/ml in all the ratios (Fig. 5.11).

The antibacterial activity for Co₃O₄ NPs with ratios 1:1, 1:2, 1:4 and 2:1 with Co-doped-ZnO 1, 4, 7 & 10 % NPs was assessed against *S. aureus*, *Shigella sonnei*, *Salmonella enterica* and *E. coli*. The antimicrobial activity of these NPs was not enhanced when using the 2mg/ml concentration of the NPs. Even after increasing the working concentration further to 15 mg/

ml, there was still no reaction. According to Vijayaragham (2010), Co_3O_4 and Co-doped-ZnO NPs did not enhance biocidal (antibacterial) activity in this study. Then more attention was now given to ZnO NPs hence it inhibited the microorganisms at the lower concentration.

The ZnO NPs results obtained from this research agree with those obtained by Zang *et al.* (2008), who reported that the ZnO bactericidal property in *E. coli*, *Salmonella typhi*, *Bacillus subtilis* and *Staphylococcus aureus*. The mechanistically bactericidal behavior of ZnO and Co-doped-ZnO might be due to chemical interactions between nanomaterials and membrane proteins and formation of free radicals from lipid bi-layers in the presence of ZnO particles (Oves *et al.* 2015; Saravanan *et al.* 2015).

The MIC results obtained from the present study showed that ZnO was mostly effective against Gram- positive bacterium (*S. aureus*), than the Gram- negative bacteria Table 5.6. In comparison with the obtained MIC values, Vijayaragham (2010) has already reported the varying MIC values of ZnO NPs against the Gram- negative bacteria. The enhanced biocidal activity of ZnO was also reported (Vijayaragham 2010). ZnO NP surface roughness was responsible for disorganisation of both cell wall and cell membrane of the tested bacteria. The team of Applerot *et al.* (2009) has also identified the antimicrobial property of ZnO NPs due to the formation of OH and O_2 in bacterial cell. The accumulation of ZnO inside the bacterial cell leading to the membrane damage and cell death was reported by Bryner *et al.* (2006).
to the formation of OH and O_2 in bacterial cell. The accumulation of ZnO inside the bacterial cell leading to the membrane damage and cell death was reported by Bryner *et al.* (2006).

MIC results for *C. albicans* and *A. niger*

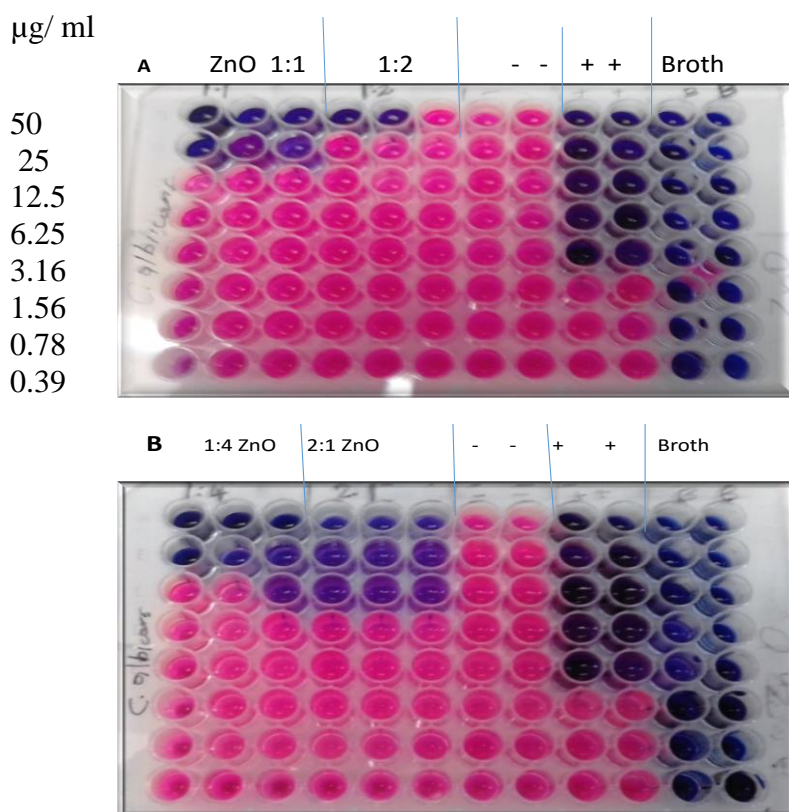


Figure 5.14. MIC results for *C. albicans* against ZnO NPs using ratio 1:1, 1: 2, 1:4 and 2:1

MIC plates after 24 hrs of incubation in modified resazurin assay. Pink color indicates growth, blue symbolizes inhibition of growth. Column 1-6 (C1-6) ZnO NPs, C (7-8) negative control, C (9-10) positive control (Amphotericin B, 2 mg/ml) and C (11- 12) broth sterility test.

In Figure 5.14, the results have revealed the ZnO NPs have antifungal activities hence it has managed to inhibit growth of *C. albicans* (Sawai and Yoshikawa 2004), in both ratio 1:1 and 1: 2 .MIC is 12.5 & 25 µg/ ml, respectively. The MIC results at ratio 1:4 and 2:1 is 12.5 & 6.25 µg/ ml, respectively. The results also show that the Amphotericin B (positive control) was more effective against *C. albicans* than ZnO nanoparticles used. The results indicate that the positive control is more susceptible to the *C. albicans* than the tested nanoparticles.

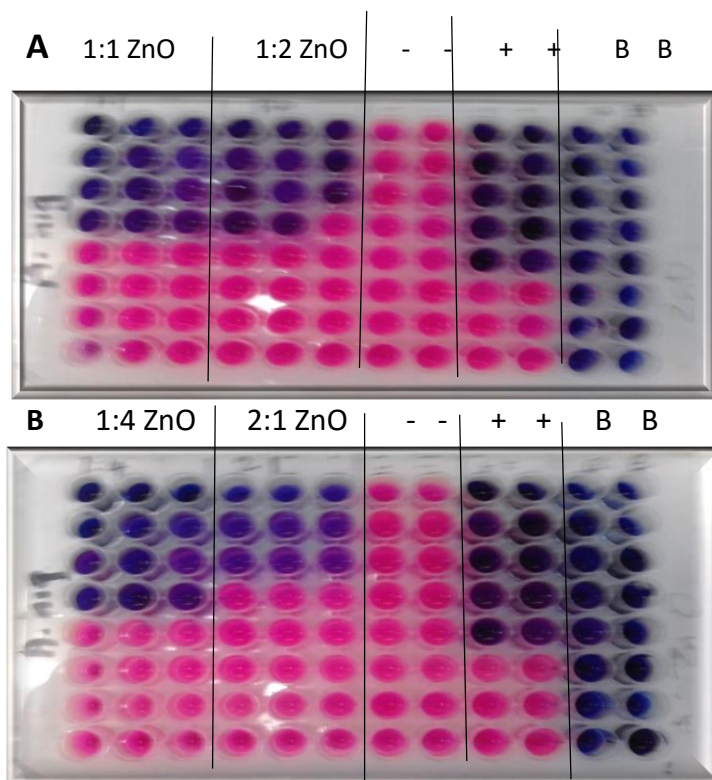


Figure 5.15. MIC results for *A. niger* and ZnO NPs, ratio 1:1, 1: 2, 1:4 and 2:1.

In Figure 5.15, the results have revealed the ZnO NPs have antifungal activities hence it has managed to inhibit growth of *A. niger* in both ratio 1:1 and 1: 2 .MIC is 3.16 $\mu\text{g}/\text{ml}$, respectively. The MIC at ratio 1:4 and 2:1 .MIC is 3.16 & 6.25 $\mu\text{g}/\text{ml}$, respectively (He *et al.* 2010). The results also show that the Amphotericin B (positive) control was more effective than ZnO nanoparticles used. The results indicate that the positive control is more susceptible to the *A. niger* than the tested nanoparticles. All the MIC concentrations for the fungal strains are recorded in Table 5.7 below.

TABLE 5.7: MIC values of synthesized ZnO at different ratios against *C. albicans* and *A. niger*

		MIC values (µg/ml)	
		Yeast	Mould
Sample name	Ratio	<i>C. albicans</i>	<i>A. niger</i>
ZnO	1:1	12.5	3.125
ZnO	1:2	25	3.125
ZnO	1:4	6.25	3.125
ZnO	2:1	12.5	6.25

The results from the current study sheds light on one of nanoparticles and their effect on the growth of two opportunistic fungi, *Aspergillus niger* and *Candida albicans*. These fungi are considered as an opportunistic pathogens that cause serious diseases in the chest (AL- Qattan 2009). In 2015, Jasim demonstrated that the ZnO nanoparticles have antifungal effects on fungal and yeast growth. The antifungal activity revealed that the growth of *A. fumigatus* and *Candida albicans* were inhibited at concentrations of 3 to 12 mg/ml of ZnO NPs.

This fact reported by He *et al.* (2010) which show that ZnO NPs show a great enhancement in the antifungal activity due to their unique properties. Sawai and Yoshikawa (2004) reported the minimum inhibitory concentration of ZnO powder against *Saccharomyces cerevisiae*, *Candida albicans*, and *Aspergillus niger* was over 100 mg/ml (~ 1.2 mol/L), whereas in this study *Candida albicans* has MIC concentration of 12.5 µg/ml and *Aspergillus niger* 6.25 µg/ml. Add to that, the inhibitory effect is not limited to the growth inhibition, but it could be the influence of nanoparticles on some of virulence factors of the yeast. Phospholipase is one of

Candida species virulence factors which has a significant role in the pathogenesis of infections and invasion of mucosal epithelia.

Furthermore, several studies have shown that clinical isolates of *Candida* have higher levels of extracellular phospholipase activity (Mahmoudabdi *et al.* 2010). Also, extracellular lipase have been proposed to the potential virulence factors of *Candida* (Schaller Schaller *et al.* 2005). Their results had shown that the ZnO NPs effect clearly on produced of these enzymes.

5. 3. TOXICITY TEST

Toxicity of nanoparticles (ZnO, Co₃O₄ and Co-ZnO) against *Daphnia magna* was investigated to establish the concentration of NPs that cause a toxicity effect to *Daphnia magna*. This has implications on loading NPs into environment and aquatic life. Figures 5.14, 5.15 and 5.16. Are the EC50 results for ZnO, Co₃O₄ and Co-ZnO against *Daphnia magna*. EC50 is the effective concentration needed to immobilise 50% of neonates. The EC50 values were estimated statistically from the fitted dose response sigmoidal curve.

Effect score

$\frac{\text{Total number of immorbilesd cells (neonates)}}{20} \times 100$

20 (Total neonates used in each concentration)

$\frac{10 \text{ cells}}{20} \times 100$

20

= 50 % Effect

EC50 is the effective concentration used early in the discovery process to evaluate the suitability and performance of drugs. It is the response corresponding to the 50 % control (Sebaugh 2010).

24h EC50 is 0.5 mg/ml

48h EC50 is 0.25 mg/ml

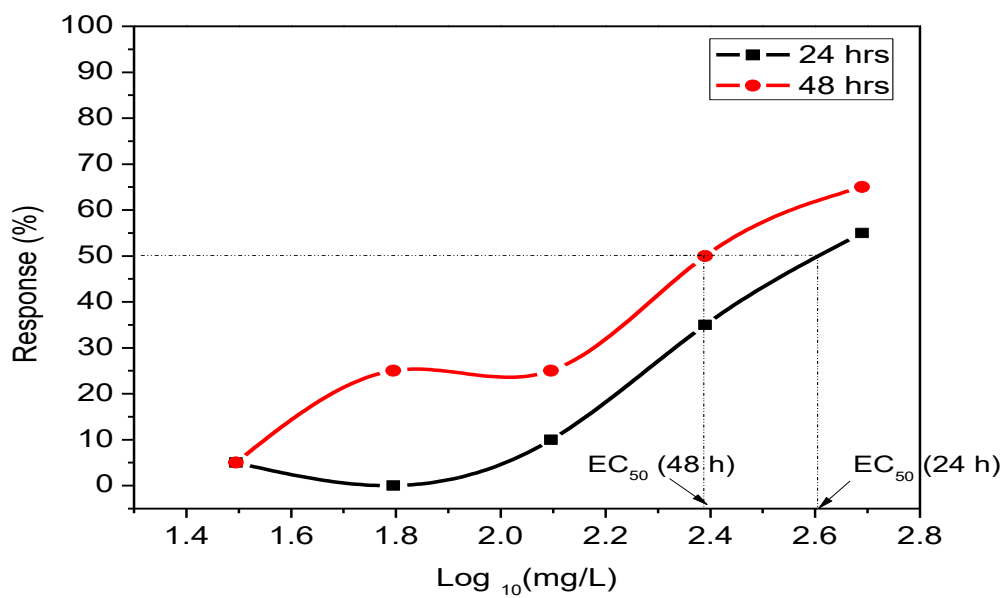


Figure 5.14: Predicted mortality at 24 and 48 h of exposure for ZnO NPs.

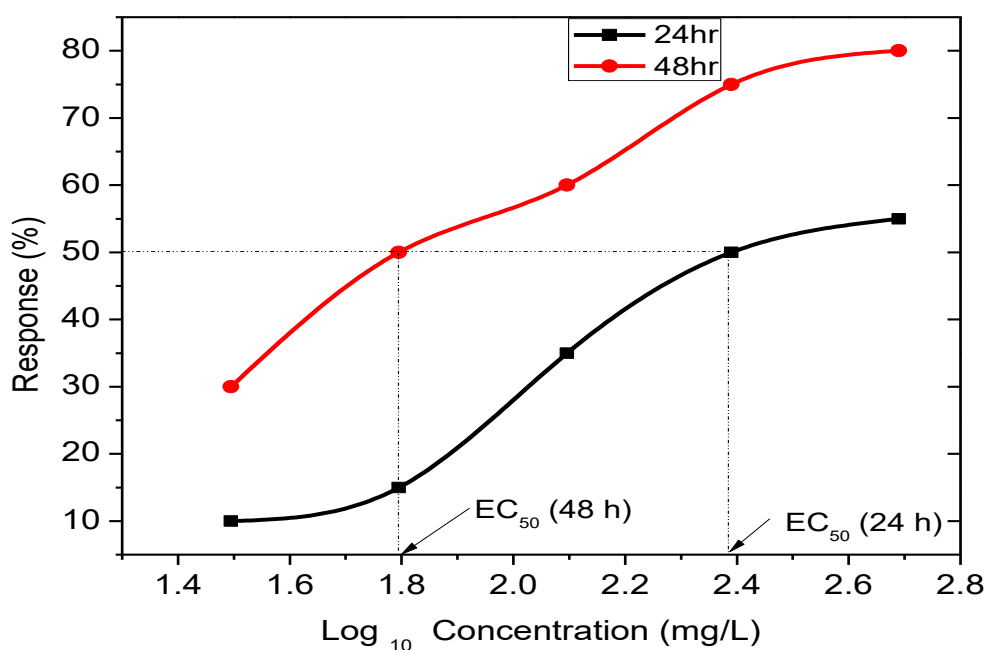


Figure 5.15: Predicted mortality at 24 and 48 h of exposure for Co₃O₄ NPs.

A number of factors affecting the hatching yield at a given day length such as temperature, light intensity, oxygen concentrations, salinity level and food quality have been investigated by several researchers (Haghpourast *et al.* 2012). In the present study the effect of ZnO (ratio 1:4), Co₃O₄ (ratio1:4) and Co- ZnO (4 %) nanoparticles *Daphnia* neonates have been observed after 24 and 48 hrs after being in stored in the dark in a cool cupboard.

Figure 5.14 shows the analysis of *Daphnia* mortality rate in two different incubation periods (24 and 48 hrs) for different concentrations of ZnO NPs. The 24 hrs EC₅₀ is found to be 0.5 mg/ml and 48 hrs EC₅₀ is 0.25 mg/ml.

The results reported for ZnO NPs indicate that the concentration time-response surfaces obtained in this study were useful and were able to extract much of the information provided in acute *Daphnia* toxicity tests. Furthermore, by using the percentage mortality models to values between 5 and 85% mortality (i.e., EC₅–LC₈₀), model adequacy was obtained (Barata,

Baird and Markich 1999). The toxicity was sometimes increasing as the exposure period is prolonged. Mortality was markedly affected at exposure periods longer than 48 h, which is the recommended standard *Daphnia* endpoint (OECD 1997).

Figure 5.15 shows the analysis of *Daphnia* mortality rate in two different incubation periods (24 and 48 h) for different concentrations of Co_3O_4 NPs. The 24 h EC_{50} is found to be 0.5 mg/ml and 48 h EC_{50} is 0.25 mg/ml and 48h EC_{50} is 0.0625 mg/ml. The Co_3O_4 NPs are found to be less toxic than ZnO hence their 48 h EC_{50} is 0.0625 mg/ml. The results reported in Figure 5.15 (Co_3O_4 NPs) indicate that the concentration time-response surfaces obtained in this study were useful and were able to extract much of the information provided in acute *Daphnia* toxicity tests. The graph indicate the gradual increase in the mortality rate as the exposure time is prolonged to 48 hrs. Furthermore mortality was markedly affected at exposure periods longer than 24 hrs, which is the recommended standard *Daphnia* endpoint (Barata *et al.* 1999)

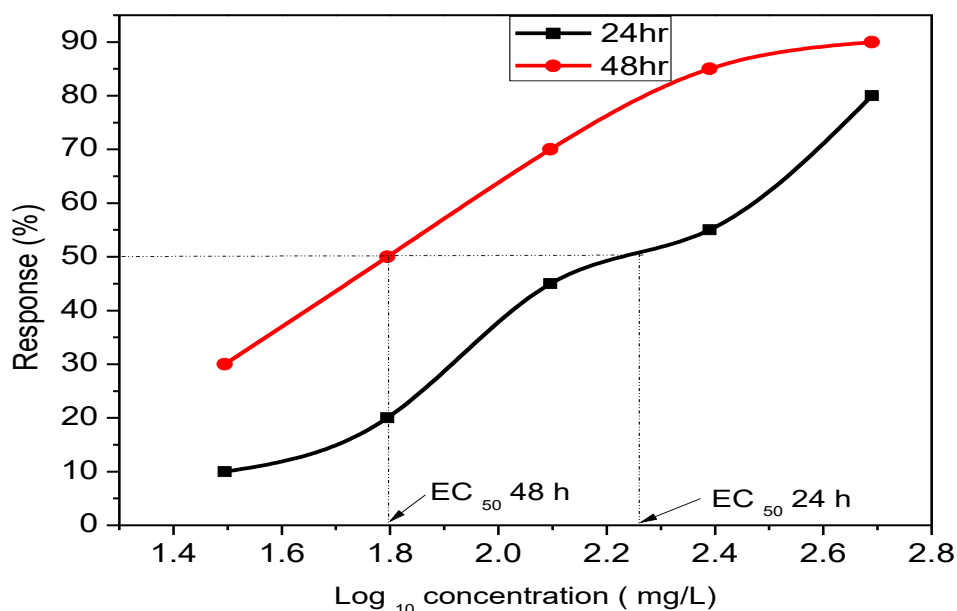


Figure 5.16: Predicted mortality at 24 and 48 h of exposure for Co-ZnO NPs.

Figure 5.16 shows the analysis of *Daphnia* mortality rate in two different incubation periods (24 and 48 hrs) for different concentrations of Co- ZnO NPs. The 24 hrs EC₅₀ is found to be 0.5 mg/ml and 48 hrs EC₅₀ is 0.25 mg/ml and 48h EC₅₀ is 0.0625 mg/ml. The results reported in Figure 5.16 where there Co- ZnO NPs are used, indicate that the concentration time-response surfaces obtained in this study were useful and were able to provide information in acute *Daphnia* toxicity tests. The toxicity was increasing as the exposure period is prolonged, as indicated by the percentage lethality graph. Mortality was markedly affected at exposure periods longer than 24 hrs. The Co- doped ZnO NPs and Cobalt oxide nanoparticles are less toxic to *Daphnia magna* than ZnO NPs.

Therefore, to credibly extrapolate from acute to chronic scenarios, longer exposures should be selected. In the present study, an optimal exposure period of 48 hrs was shown to have less effects on mortality thresholds and low concentration.

CHAPTER 6

CONCLUSION AND RECOMMENDATION

Chapter Six provides the general conclusion and recommendations.

CONCLUSIONS

The aim of the study was to synthesise and characterise cobalt doped zinc oxide nanoparticles; assessment of their antimicrobial activity against selected waterborne pathogens. The composites were successfully prepared and confirmed by various characterization techniques. They were also assessed for their antimicrobial activity using the disc diffusion and MIC method. Then a toxicity then was done using the Daphtokit.

The following conclusions were drawn from the study:

The synthesis zinc oxide nanoparticles was successfully prepared using microwave-assisted synthesis method. Composites were produced in short reaction time, where the method was user friendly and the reproducibility of the composites was obtained. For the synthesis of cobalt oxide (Co₃O₄) nanoparticles, mechanochemical method was chosen. The precipitate was pink but turned black after being calcined and nanoparticles were formed. The synthesis of Co- ZnO nanoparticle was successfully prepared using the reflux and blue solid was obtained from pink cobalt ion solution.

Operating parameters such as temperature, power, time and precursor concentration were found to have an influence on the resulting composites; therefore, the conditions were optimized for reproducibility and to match the performance properties of the composites.

The antimicrobial activity of the composites was first studied using the inhibition

zone/ agar well diffusion method and followed by MIC method. Bacterial strains: *Salmonella enterica*, *Escherichia coli*, *Shigella sonnei* and *Staphylococcus aureus*, yeast and mould, *Candida albicans* and *Aspergillus niger*. The well diffusion results showed that the ZnO and Co-ZnO NPs gave a higher inhibition zones against *S. aureus* and slight inhibition against *A. niger* at a concentration of 30 mg/ml. The high inhibition effect suggested that the NPs exerted a stronger antimicrobial activity on the organism and is therefore a potential to use as an inhibition growth material for bacteria and moulds. Co₃O₄ NPs did not show any zones of inhibition for all the organisms used.

When ZnO NPs was applied to microorganisms through MIC, it was effective and potent antimicrobial agent against waterborne pathogens. MIC varied from 6.25- 25 µg/ml for all selected bacteria and varied between 3.125- 25 for fungal strains. Co₃O₄ and Co- ZnO NPs did not inhibit growth at all.

As reviewed from open source literature, these results are attributed to the small sizes of the nanoparticles, where the size of nanoparticles plays a major role in the inactivation of bacteria and fungi.

A disadvantage with the prepared clay composites is that, they cannot be poured directly into the water in their powder form and be used as an antibacterial material. This is because of the many side effects associated with the nanoparticles and their small sizes. Some of them could be harmful to aquatic environment and human consumption. Therefore, toxicity test is necessary which is promising to deliver the intended properties of the NPs.

When the toxicity studies were performed using DAPHTOXKIT F, results showed that Co-ZnO NPs is less toxic to *Daphnia magna* compared to ZnO and Co₃O₄ NPs.

RECOMMENDATION

The application of Co- ZnO NPs as a potential decontamination agent is recommended in future studies. Though it has inhibited the growth of bacteria at a high level of concentration, still it has showed antimicrobial effect in disk diffusion method. When toxicity tests were done for all synthesised NP, Co- ZnO NPs has shown less toxicity to *Daphnia magna* than other tested NPs. The future studied will probably witness important novel developments applied nanoresearch regarding antimicrobial agent.

Either than *Daphnia magna*, other crustaceans/ zooplanktons can be used in future research studies to ensure the environmental safety onto the selected NPs

CHAPTER 7

REFERENCES

Chapter Seven is the list of all references used to compile the study.

ABDELHAY, A., CARMEN-MIHAELA, T., CHRISTOPHE, M., CEDRIC, M., HÉLÈNE, G., GHOUTI, M., RAPHAEL, S. (2012). Physicochemical properties and cellular toxicity of (poly) aminoalkoxysilanes-functionalized ZnO quantum dots. *Nanotechnology*, 23, pp. 335101.

ALIAS, S. S., ISMAIL, A. B. and MOHAMAD, A. A. (2010). Effect of pH on ZnO nanoparticle. *Annual Review of Microbiology*, 60, pp. 397–423.

ALL AFRICA. (2014). Available at: <http://allafrica.com/stories/201210081462.html>. Accessed December 2014.

ALLAHVERDIYEV, A. M., KON, K. V., ABAMOR, E. S., BAGIROVA, M. and RAFAILOVICH, M. (2011). Coping with antibiotic resistance: combining nanoparticles with antibiotics and other antimicrobial agents. *Expert Review of Anti-Infective Therapy*, 9, pp. 1035-1052.

ANNESH, P. M., CHERIAN, C.T., JAYARAJ, M. K., ENDO, T. (2010). Co²⁺ doped ZnO nanoflowers grown by hydrothermal method. *Journal of Ceramic Society of Japan*, 118, pp. 333–336.

ATHAR, T., HAKEEM, A., TOPNANI, N. and HASHMI, A. 2012. Wet Synthesis of Monodisperse Cobalt Oxide Nanoparticles. *Journal of Nanomaterials*, 1, pp. 1-5.

APPLEROT, B.G., LIPOSVK, A., DROR, R., PERKAS, N. NITZAN, Y., and LUBART, R. 2009. *Advanced Functional Material*, 19, pp. 842.

AMERICAN PUBLIC HEALTH ASSOCIATION (APHA). (1998). Standard Methods for the Examination of Water and Wastewater. 20th Edition, American Public Health Association, American Water Works Association and Water Environmental Federation, Washington DC.

BAE, D. S., KIM, E. J., BANG, J. H., KIM, S. W., HAN, K. S., LEE, J. K., KIM, B. I. and ADAIR, J. H. (2005). Synthesis and characterization of silver nanoparticles by a reverse micelle process. *Journal of Metals and Materials International*, 4, pp. 291–294.

BARATA, C., BAIRD, D. J., AND MARKICH, S. J. (1999). Comparing Metal Toxicity among *Daphnia magna* Clones: An Approach Using Concentration-Time-Response Surface. *Archives of Environmental Contamination and Toxicology*, 37, pp. 326–331

BASITH, N. M., VIJAYA, J. J., KENNEDY, L. J., BOUOUDINA, M. JENEFAR, S. and KAVIYARASAN, V. (2014) Co-doped ZnO nanoparticles: Structural, morphological, optical, magnetic and antibacterial studies. *Journal of Materials Science and Technology*, 30, pp. 1108–1117.

BLINOVA, I. (2000). Use of bioassays for toxicity assessment of polluted water. Institute of Environmental Engineering at Tallinn Technical University.

BOUCHARD, L. S., ANWAR, M. S., LIU, G. L., HANN, B., XIE, Z. H., GRAY, J. W., WANG, X., PINES, A. and CHEN, F. F. (2009). Picomolar sensitivity MRI and photoacoustic imaging of cobalt nanoparticles. *Proceedings of the National Academy of Sciences of the United States of America*, 106, pp. 4085-4089.

BRAYNER, R., FERRARI-ILIOU, R., BRIVOIS, N., DJEDIAT, S., BENEDETTI, M.F. and FIEVET, F. (2006). Toxicological impact studies based on Escherichia coli bacteria in ultrafine ZnO nanoparticles colloidal medium. *Nano Letters*, 6, pp. 866–870.

BRINKER C. J. and SCHERER G. W. (1990). Sol gel science: The physics and chemistry of of sol-gel processing. *Academic press*. ISBN 0-12-134970-5. Accessed November 2014.

CABRAL, J. P. S. (2010). Water Microbiology. Bacterial pathogens and water. *International Journal of Environmental Research and Public Health*, 7, pp. 3657–3703.

CANPOLAT, E. and KAYA, M. (2004). Synthesis, characterization of some Co(III) complexes with vic-dioxime ligands and their antimicrobial properties. *Turk. Journal of Chemistry*, 28, pp. 235–242.

CHANG, E. L., SIMMERS, C. and KNIGHT, D. A. (2010). Review Cobalt Complexes as Antiviral and Antibacterial Agents. *Center for Bio/Molecular Science and Engineering*, Naval Research Laboratory.

CHANDRA, S. and KUMAR, A. (2012). Synthesis and characterisation of copper nanoparticles by reducing agent. *Journal of Saudi Chemical Society, Original article*, pp. 150- 153.

CHOI, S. H. and LEE, H. (2004). “Optical Characterization of Si Nanocrystals in Si-rich SiO_x and SiO_x/SiO₂ Multilayers Grown by Ion Beam Sputtering”, *Journal of the Korean Physics Society*, 45, pp. 116.

COMMON METHODS OF WATER DISINFECTION. (2014). Available at:

<https://www.filtersfast.com/articles/Common-Methods-of-Water-Disinfection.php>.

- CORRIU, R. and ANH, N. T. (2009). Molecular chemistry of sol-gel derived nanomaterials. *John Wiley and Sons*. ISBN 0-470-72117-0. Accessed November 2014.
- CRUICKSHANK, R. (1968). Medical microbiology: A guide to diagnosis and control of infection. 11th (ed), Edinburgh and London: E&S. Livingston Ltd., pp. 888.
- DEMOCRATIC REPUBLIC OF CONGO. (2014.) A diagnostic of water, sanitation, hygiene and poverty in the DRC. World Bank Group.
- EASTOE, J., HOLLAMBY, M. J. and HUDSON, L. (2006). Recent advances in nanoparticle synthesis with reversed micelles. *Advances in Colloid and Interface Science*, pp. 128–130, 5–15.
- ECCE'10/ECCIE'10/ECME'10/ECC'10. (2015). Proceedings of the European Conference of Chemical engineering, and European conference of civil engineering, and European conference of mechanical engineering, and European conference on Control, pp. 88–94.
- EMCH, M., ALI, M. and YUNUS, M. (2008). Risk areas and neighborhood-level risk factors for *Shigella dysenteriae* 1 and *Shigella flexneri*. *Health Place*, 14, pp. 96–105.
- FABBIYOLA, S., KENNEDY, L. J., ARULDOSS, U., BOUOUDINA, M., DAKHEL, A. A. and JUDITHVIJAY, J. (2015). Synthesis of Co-doped ZnO nanoparticles via co-precipitation: Structural, optical and magnetic properties. *Powder Technol.* 286, pp. 757–765.
- FARHADI, S., SAFABAKHSH, J. and ZARINGHADAM, P. (2013). Synthesis, characterisation and investigation of optical and magnetic properties of cobalt oxide (Co₃O₄) nanoparticles. *Journal of Nanostructure in Chemistry*, 3, pp. 69.
- GALLO, J., HOLINKA, M. and MOUCHA, C. S., (2014). Antibacterial Surface Treatment for Orthopaedic Implants. *Journal of Molecular Science*, 5(18), pp. 13849- 13880.

GEDYE, R. N., SMITH, F. E. and WESTAWAY, K. C. (1988). The rapid synthesis of organic com-pounds in microwave ovens. *Canadian Journal of Chemistry*, 66, pp. 17–26.

GOSMANN, H. and FELDMANN, C. (2010). Synthesis and characterization of inorganic nanoparticles, *Angrew chemistry*, 49, pp. 1362 - 1395.

GUZMÁN, M. G, DILLE, J. and GODET, S. (2009). Synthesis of silver nanoparticles by chemical reduction method and their antibacterial activity. *International Journal of Chemical and Biomolecular Engineering* 2(3), pp. 108.

HADZIC, B., ROMCEVIC, N., ROMCEVIC, M., KURLISZYN- KUDELSKA, I., DOBROWOLSKI, W., TRAJIC, J., TIMOTIJEVIC, D., NARKIEWICZ, U. and SIBERA, D. (2012). Surface optical phonons in ZnO(Co) nanoparticles: Raman study. *Journal of Alloys and Compounds*, 540, pp. 49–56.

GLOBAL SYSTEM FOR MOBILE COMMUNICATION (GSM). (1989). Available at: <http://www.iec.org>. GSM 1989, The International Engineering Consortium.

HAGHPARAST, S., SHABANI, A., SHABANPOUR, B. AND HOSEINI, S. A. (2012). Hatching Requirements of *Daphnia magna* Straus, 1820, and *Daphnia pulex* Linnaeus, 1758, Diapausing Eggs from Iranian Populations. *In Vitro. Journal of Agriculture and Science Technology*, 14, pp. 811-820.

HAIPOUR, M.J., FROMM, K. M., ASHKARRAN, A. A. and DEABERASTURI, D. J. (2012). Antibacterial properties of nanoparticles. *Trends in biotechnology*, 10, pp. 1016- 1019.

HAMMAD, T. M., SALEM, J. K. and HARRISON, R. G. (2012). Structure, optical properties and synthesis of Co-doped ZnO Superstructures. *Applied nanosciences*, pp. 1- 8.

HE, L., LIU, Y., MUSTAPHA, A., and LIN, M., (2011). Antifungal activity of zinc oxide nanoparticles against *Botrytis cinerea* and *Penicillium expansum*. *Microbiological Research*, 166, pp. 207-215.

HUANG, Z., ZHENG, X., YAN, D., YIN, G., LIAO, X. and KANG, Y. (2008). Toxicological effect of ZnO nanoparticles based on bacteria. *Langmuir*. 24, pp. 4140- 4144.

IVILL, M., PEARTON, S. J., RAWAL, S., LEU, L., SADIK, P., DAS, R., HEBARD, A. F., CHISHOLM, M., BUDAI, J. D. and NORTON, J. D. (2008). Structure and magnetism of cobalt-doped ZnO thin films. *New Journal of Physics*. 10, pp. 065.

JAFARI, F., SHOKRZADE, L., HAMIDIAN, M., SALMANZADEH-AHRABI, S., ZALI, M. R. (2008). Acute diarrhea due to enteropathogenic bacteria in patients at hospitals in Tehran. *Japanese Journal of Infectious Diseases*, 61, pp. 269–273.

JAYAKUMAR, O. D., SUDARSAN, V. and TYAGI, A. K. (2015). Bifunctional Li and Co doped ZnO nanostructures synthesized by solvothermal method: Stabilizer controlled shape and size tuning. *Journal of Nanoscience and Nanotechnology*, 15, pp. 2804–2809.

JOSHI, M., BHATTACHARYYA, A. and ALI, S. W. (2008). Characterization Techniques for Nanotechnology Applications in Textiles. *Indian Journal of Fibre and Textile Research*, 3, pp. 304 -317.

JURABLU, S., FARAHMANDJOU, M. and FIROOZABADI, T. P. (2015). Sol-Gel Synthesis of Zinc Oxide (ZnO) Nanoparticles: Study of Structural and Optical Properties. *Journal of Sciences, Islamic Republic of Iran*, 26(1), pp. 281 – 285.

KAPPE, C.O. (2004). Controlled Microwave Heating in Modern Organic Synthesis. *Angewandte Chemie International Edition*, 43, pp. 6250–6284.

KARVANI, Z. E., CHEHRAZI, P. (2011). Antibacterial activity of ZnO nanoparticle on gram-positive and gram-negative bacteria. *African Journal of Microbiology Research*, 5, pp. 1368-1373.

KAUSHIK, A., DALELA, B., RATHORE, R., VATS, V. S., CHOUDHARY, B. L., ALVI, P. A., KUMAR, S. and DALELA, S. (2013). Influence of Co doping on the structural,

optical and magnetic properties of ZnO nanocrystals. *Journal of Alloys and Compounds*, 578, pp. 328–335.

KAYA, M., YENIKAYA, C., COLAK, A. T. and COLAK, F. (2008). Synthesis, spectral, thermal and biological studies of Co(III) and binuclear Ni(II) complexes with a novel amine-imine-oxime ligand. *Russian Journal of General Chemistry*, 78, pp. 1808–1815.

KHEIRALLA, Z. M. H., RUSHDY, A. A., BETIHA, M. A. and YAKOB, N. A. N. (2014). High-performance antibacterial of montmorillonite decorated with silver nanoparticles using microwave assisted method. *Journal of Nanoparticle Research*, 16, pp. 2560–2566.

KHEYBARI, S., SAMADI, N., HOSSEINI, S. V., FAZELI, A. and FAZELI, M. R. (2010). Synthesis and antimicrobial effects of silver nanoparticles produced by chemical reduction method. *DARU Journal of Pharmaceutical Sciences*, 18, pp. 168–172.

KLEIN, L. C. (1994). Sol- gel optics: Processing and applications. Rutgers, The State University of New Jersey. Published by Springer science, LLC.

KRASNER, S. W., WEINBERG, H. S., RICHARDSON, S. D. PASTOR, S.J., CHINN, R., SCLIMENTI, M.J., ONSTAD, G.D. and THRUSTON Jr., A. D. (2006). Occurrence of a new generation of disinfection by-products. *Environmental Science and Technology*, 40, pp. 7175–7185.

KRISHNA, R. R., RANJIT, T. K. and ADHAR, C. M. (2011). Size-Dependent Bacterial Growth Inhibition and Mechanism of Antibacterial Activity of Zinc Oxide Nanoparticles. *Langmuir*, 27, pp. 4020- 4028.

KUMAR, H. and SANGWAN, P. (2011). Synthesis and Characterization of Cobalt Oxide Nanoparticles by Sol-Gel Method. *Advances in Applied Physical and Chemical Sciences - A Sustainable Approach*, 1, pp. 99- 104.

KUMAR, H., RANI, R. and SALAR, R. (2010). Reverse micelle synthesis, characterization & antibacterial study of nickel nanoparticles.

KUO, C. Y., WONG, R. H., LIN, J. Y., LAI, J. C. and LEE, H. (2006). Accumulation of chromium and nickel metals in lung tumors from lung cancer patients in Taiwan. *Journal of Toxicology and Environmental Health*, 69, pp. 1337-1344.

KURYLISZYN-KUDELSKA, I., HADZIC, B., SIBERA, D., ROMCEVIC, M., ROMCEVIC, N., NARKIEWICZ, U., LOJKOWSKI, W., ARCISZEWSKA, M. and DOBROWOLSKI, W. (2013). Magnetic properties of ZnO(Co) nanocrystals. *Journal of Alloys Compounds*, 561, pp. 247–251.

LI, C., CHE, P., SUN, C. and LI, W. (2016). Effect of cobalt concentration and oxygen vacancy on magnetism of Co doped ZnO nanorods. *Journal of Nanoscience Nanotechnology*, 16, pp. 2719–2724.

LI, Y., LEE, E. J. and CHO, S. O. (2007). Superhydrophobic coating on curved surfaces featuring remarkable supporting force. *Journal of Physical Chemistry C*, 111, pp. 14813–14817.

LIN, D. and XING, B. (2008). Root uptake and phytotoxicity of ZnO nanoparticles. *Environmental Science and Technology*, 42, pp. 5580-5585.

LIN, S., ZHAO, Y., XIA, T, MENG H, JI, Z. and LIU, R. (2011). High content screening in zebra fish speeds up hazard ranking of transition metal oxide nanoparticles. *ACS Nanotechnology*, 5, pp. 7284-7295.

LISON, D., DE BOECK, M., VEROUGSTRAETE, V. and KIRSCH-VOLDERS, M. (2001). Update on the genotoxicity and carcinogenicity of cobalt compounds. *Occupational and Environmental Medicine*, 58, pp. 619-625.

LISON, D., LAUWERYS, R., DEMEDTS, M. and NEMERY, B. (1996). Experimental research into the pathogenesis of cobalt/hard metal lung disease, 9, pp. 1024-1028.

MAGAYE, R., ZHAO, J., BOWMAN, L. and DING, M. (2012). Genotoxicity and carcinogenicity of cobalt-, nickel- and copper-based nanoparticles. *Experimental and therapeutic medicine*, pp. 551- 561.

MAKHNIY, V. P. and MELNIK, V. V. (2003). Surface barrier diode based on zinc selenide with a passivating zinc oxide film. *Technical Physics Letters*, Springer, 29(9), pp. 712-713.

MANJULA, G. NAIR, M. NIRMALA, K. REKHA, A. and ANUKALIANI. (2011). Structural, optical, photo catalytic and antibacterial activity of ZnO and Co doped ZnO nanoparticles. *Materials Letters*, 65, pp.1797–1800.

MARINHO, J. Z., ROMEIRO, F. C., LEMOS. S. C. S., MOTTA, F. V., RICCARDI, C. S. and LONGO, M. (2012). Urea-Based Synthesis of Zinc Oxide Nanostructures at Low Temperature. *Journal of Nanomaterials*, 1, pp. 1-7.

MARTÍNEZ, B., SANDIUME SANDIUMENGE, F., BALCELLS, L. I., ARBIOL, J., SIBIEUDE, F. and MONTY, C. (2005). Structure and magnetic properties of Co-doped ZnO nanoparticles. *Physics Review Journals*, 72, pp. 165-202.

METHODS OF WATER DISINFECTION. 2014. Available at:
<https://www.waterchlorine.com>. Accessed November 2014.

MIYAWAKI, J., YUDASAKA, M., IMAI, H., YORIMITSU, H., ISOBE, H., NAKAMURA, E. and IJIMA, S. (2006). In vivo magnetic resonance imaging of single-walled carbon nanohorns by labeling with magnetite nanoparticles. *Advanced Materials*, 18, pp. 1010–1014.

NAIR, M. G., NIRMALA, M., REKHA, K. and ANUKALIANI, A. (2011). Structural, optical, photo catalytic and antibacterial activity of ZnO and Co doped ZnO nanoparticles. *Material Letters*, 65, pp. 1797–1800.

NATIONAL DRINKING WATER CLEARINGHOUSE fact sheet. Disinfection. (1996).

Available at:

http://www.nesc.wvu.edu/pdf/dw/publications/ontap/2009_tb/disinfection_dwfsom50.pdf.

Accessed January 2015.

NAVALE, G. R., THIRIPURANTHAKA, M., LATE, D. J. and SHINDE, S. S. (2015).

Antimicrobial Activity of ZnO Nanoparticles against Pathogenic Bacteria and Fungi. *JSM Nanotechnology and Nanomedicine*, 3(1), pp. 1033 – 1035.

NUCHTER, M., ONDRUSEHKA, B., BONRETH, W. and GUM, A. (2004). Microwave assisted synthesis – a critical technology overview. *Green Chemistry*, 6, pp. 128–141.

ORGANIZATION FOR ECONOMIC CO- OPERATION AND DEVELOPMENT (OECD).

(1997). Report on Regulatory Reform Synthesis. Paris.

OLDING, T., SAYER, M. and BARROW, D. (2001). Ceramic sol-gel composite coatings for electrical insulation. *Thin Solid Films*, pp. 398-399; 581–586.

OVES, M., ARSHAD, M., KHAN, M. S., AHMED, A. S., AZAM, A. and ISMAIL, I. M. (2015). Anti-microbial activity of cobalt doped zinc oxide nanoparticles: Targeting water borne bacteria. *Journal of Saudi Chemical Society*, 3, pp. 581- 590.

PAL, B. and GIRI, P. K. (2011). Defect mediated magnetic interaction and high T_c Ferromagnetism in Co doped ZnO nanoparticles. *Journal of Nanotechnology*, 10, pp. 9167- 74.

PANACEK, A., KOLA, M., VECEROVA, R., PRUCEK, R., SOUKUPOVA, J., KRYSTOF, V., HAMAL, P., and KVITEK, L. (2009). Antifungal activity of silver nanoparticles against *Candida* spp. *Biomaterials*, 30, pp. 6333 – 6340.

PARK, J. H., KIM, M.G., JANG, H. M., RYU, S. and KIM, Y. M. (2004). Co-metal clustering as the origin of ferromagnetism in Co-doped ZnO thin films. *Applied Physics Letters*, 84, pp.1338–1340.

- PRABHU, N., DIVYA, T. R. and YAMUNA, G. (2010). Synthesis of silver phyto nanoparticles and their antibacterial efficacy. *Digest Journal of Nanomaterials and Biostructures*, 5, pp. 185-189.
- RADU, G. L., TRUICA, G. I., PENU, R. MOROEANU, V. and LITESCU, S.C. (2012). Use of the Fourier Transform Infrared Spectroscopy in Characterization of Specific Samples. *U.P.B. Scientific Bulletin*, 74(4), pp. 139.
- RALIYA, R., SARAN, R., CHOUDHARY, K. and TARAFDAR, J. (2013). Biosynthesis and Characterization of Nanoparticles. *Journal of Advancement in Medical and Life Sciences*, 1(1), pp. 2-6.
- RAMGIR, N. S., LATE, D. J., BHISE, A. B., MORE, M. A., MULLA, I. S. and JOAG, D. S. (2006). ZnO Multipods, Submicron Wires, and Spherical Structures and Their Unique Field Emission Behavior. *The Journal of Physical Chemistry B*, 110, pp. 18236-18242.
- RAO, Y. N., BANERJEE, D., DATTA, A., DAS, S. K., GUIN, R. and SAHA, A. (2010). Gamma irradiation route to synthesis of highly re-dispersible natural polymer capped silver nanoparticles Radiate. *Physical Chemistry*, pp. 791240–6.
- REKHA, K., NIRMALA, M., NAIR, M. G. and ANUKALIANI, A. (2010). Structural, optical, photocatalytic and antibacterial activity of zinc oxide and manganese doped zinc oxide nanoparticles. *Physics B*, 405, pp. 3180–5.
- RICHARDSON, S. D. (2003a). Disinfection by-products and other emerging contaminants in drinking water. *Trends in Analytical Chemistry*, 22, pp. 666–684.
- RICHARDSON, S. D. (2003b). Water analysis: Emerging contaminants and current Issues. *Analytical Chemistry*, 75, pp. 2831–2857.

RICHARDSON, S. D. (2004). Environmental mass spectrometry: Emerging contaminants and current issues. *Analytical Chemistry*, 76, pp. 3337- 3364.

RUKMINI, I. K. and SUVARNALATHA, D. P. (2011). Antimicrobial activity of Silver Nanoparticles synthesized by using Medicinal Plants. *International Journal of ChemTech Research*, 3(3), pp. 1394 -1402.

SABAHI, J. A., BORA, T., ABRI M. A. and DUTTA, J. (2016) .Controlled Defects of Zinc Oxide Nanorods for Efficient Visible Light Photocatalytic Degradation of Phenol. *Materials*, MDPI, 9(4), pp. 238.

SADJADI, M. S., POURAHMAD, A., SOHRABNEZHAD, S. H. and ZARE, K. (2006). Formation of NiS and CoS semiconductor nanoparticles inside mordenite-type zeolite. 61, pp. 2923-2926.

SALAVATI-NIASARI, M. KHANSARI, A. and DAVAR, F. (2009). Synthesis and characterization of cobalt oxide nanoparticles by thermal treatment process. *Inorganica Chimica Acta*, 362, pp. 4937–4942.

SARAVAN, S. and VIJAYAKUMAR, S. (2015). Bio-surfactants Type, Sources and Applications. *Research Journal of Microbiology*, 10, pp. 181- 192.

SAVITHRAMMA, N., RAO, M. L., K. RUKMINI, I. K. and SUVARNALATHA DEVI, P., (2011). Antimicrobial activity of Silver Nanoparticles synthesized by using Medicinal Plants. *International Journal of ChemTech Research*, 3(3) pp. 5- 6.

SCOTT, J. R. and BARNETT, T. C. (2006). Surface proteins of gram-positive bacteria and how they get there. *Annual Review of Microbiology*, 60, pp. 397- 423.

SEBAUGH. (2010). Guidelines for acute EC50/IC50 estimation. *Pharmaceutical statistics*, 10, pp. 128- 134.

SHAHEEN, T. H., NAGGAR, M.E., ABDELGAWAD, A. M. and HEBEISH, A. (2016). Durable antibacterial and UV protections of in situ synthesized zinc oxide nanoparticles onto cotton fabrics. *International Journal of Biological Macromolecules*, 83, pp. 426–432.

SHI, T. and ZHU, S. (2007). Structures and magnetic properties of wurtzite $Zn_{1-x}Co_xO$ dilute magnetic semiconductor nanocomposites. *Applied Physics Letters*, 90, pp. 102-108.

SHI, T., XIAO, Z., YIN, Z., LI, X., WANG, Y., HE, H., WANG, J., YAN, W. and WEI, S. 2010. The role of Zn interstitials in cobalt-doped ZnO diluted magnetic semiconductors. *Applied Physics Letters*, 96, pp. 211.

SHIVANANDA, C. S., ASHA, S., MADHUKUMAR, R., SATISH, S., NARAYANA, B., BYRAPPA, K., WANG, Y. and SANGAPPA, Y. (2016). Biosynthesis of colloidal silver nanoparticles: their characterization and antibacterial activity.

SOLOMON, P., BAUMANN, K, EDGERTON, E., and TANNER. R. (1998). Comparing of integrated samplers for mass and composition during the 1989 Atlanta supersites project. *Journal of Geophysical Research*, 108(7), pp. 23.

SONDI, I. and SALOPEK-SONDI, B. (2004). Silver nanoparticles as antimicrobial agent: A case study on E. coli as a model for gram negative bacteria. *Journal of Colloid and Interface Science*, 275, pp. 177–182.

SOURABH, D., RIZWAN. W., FARHEEN, K., YOGENDRA, K. M., JAVED, M., and ABDULAZIZ, A. A. (2014). Reactive Oxygen Species Mediated Bacterial Biofilm Inhibition via Zinc Oxide Nanoparticles and Their Statistical Determination. *PLOS ONE*, 9, pp. 111-130.

STUART, B. (2005). Infrared Spectroscopy. *Kirk-Othmer Encyclopedia of Chemical Technology*. (Wiley Online Library).

SWAPP, S. (2012). Scanning electron microscopy (SEM). *Geochemical Instrumentation and Analysis*.

TANG, Z. X. and BIN-FENG, L. (2014). MgO nanoparticles as antibacterial agent: preparation and activity. *Brazilian Journal of Chemical Engineering*, 31(3), pp. 591 – 601.

THILL, A. (2006). Cytotoxicity of CeO₂ nanoparticles for Escherichia coli. Physico-chemical insight of the cytotoxicity mechanism. *Environmental Science and Technology*, 40, pp. 6151–6156.

UIKEY, P. and DR. VISHWAKARMA, K. (2016). Nanotechnology Department, Review Of Zinc Oxide (ZnO) Nanoparticles Applications and Properties. *International Journal of Emerging Technology in Computer Science & Electronics*, 21(2), pp. 239.

VACCINE NEWS DAILY. (2014). Available at: <http://vaccinenewsdaily.com/africa/320429-cholera-outbreak-in-sierra-leone-slows/>. Accessed December 2014.

WANG, K., XU, J. J. and CHEN, H. Y. (2005). A novel glucose biosensor based on the nanoscaled cobalt phthalocyanine-glucose oxidase biocomposite. *Biosensors and Bioelectronics*, 20, pp. 1388-1396.

WENNERAS, C. and ERLING, V. (2004). Prevalence of Enterotoxigenic Escherichia coli associated diarrhoea and carrier state in the developing world. *Journal of Health, Population and Nutrition*, 22, pp. 370–382.

WORLD HEALTH ORGANIZATION (WHO). (2015). Available at: <http://www.afro.who.int/en/ghana/news/item/6974-who-provides-technical-support-to-fight-cholera-outbreak-in-ghana.html>. WHO provides technical support to fight Cholera Outbreak in Ghana. Accessed January 2015 and http://www.who.int/water_sanitation_health/takingcharge. WHO World Water Day Report. Accessed December 2013.

WOJNAROWICZ, J., CHUDOBA, T., KOLTSOV, I., GIERLOTKA, S.,
DWORAKOWSKA, S. and LOJKOWSKI, W. (2018). Size control mechanism of ZnO nanoparticles obtained in microwave solvothermal synthesis. *Nanotechnology*, 29, pp. 65.

WOJNAROWICZ, J., OPALINSKA, A., CHUDOBA, T. GIERLOTKA, S., MUKHOVSKYI, R., PIETRZYKOWSKA, E., SOBCZAK, K. and LOJKOWSKI, W. (2016). Effect of water content in ethylene glycol solvent on the size of ZnO nanoparticles prepared using microwave solvothermal synthesis. *Journal of Nanomaterial*, pp. 2789871.

WONG, S. W., LEUNG, P. T., DJURISI, A. B., and LEUNG, K. M. (2010). Toxicities of nano zinc oxide to five marine organisms: influences of aggregate size and ion solubility. *Analytical and Bioanalytical Chemistry*, 396, pp. 609-618.

XU, X. and CAO, C. (2010). Hydrothermal synthesis of Co-doped ZnO flakes with room temperature ferromagnetism. *Journal of Alloys and Compounds*, 501, pp. 265–268.

YANG, H., HU, Y., ZHANG, X. and QIU, G. (2003). Mechanochemical synthesis of cobalt oxide nanoparticles. *Science direct*, 58, pp. 387- 389.

ZHANG, H., SHAN, Y. and DONG, L. (2014). A comparison of TiO₂ and ZnO nanoparticles as photosensitizers in photodynamic therapy for cancer. *Journal of Biomedical Nanotechnology*, 10, pp. 1450-1457.

ZHANG, P., CHAN, C. K. LI, X. G., XUE, Q. and ZHAO X. G. (2002). Dynamics of the spin-2 Bose condensate driven by external magnetic fields. *Physical Review A*, 66, pp. 043606.

ZHANG, Y. B., ALI, S. F., DERVISHI, E., XU, Y., LI, Z. R., and CASCIANO, D. (2010). Cytotoxicity effects of graphene and single-wall carbon nanotubes in neural pheochromocytoma-derived PC12 cells. *ACS Nanotechnology*, 4, pp. 3181-3186.

ZHAO, X., ZHOU, R., HUA, Q., DONG, L., YU, R. and PAN, C. (2015). Contacted ZnO Nanowire Sensors, *Journal of Nanomaterials*, Hindawi, pp. 20.